SDPRX: A statistical method for cross-population prediction of complex traits

Authors

Geyu Zhou, Tianqi Chen, Hongyu Zhao

Correspondence

hongyu.zhao@yale.edu

We developed a statistical method, SDPRX, to improve the performance of polygenic risk score (PRS) in non-European populations by jointly modeling GWAS summary statistics from European and non-European populations.

SDPRX: A statistical method for cross-population prediction of complex traits

Geyu Zhou,[1,2] Tianqi Chen,[2] and Hongyu Zhao[1,2,*]

Summary

Polygenic risk score (PRS) has demonstrated its great utility in biomedical research through identifying high-risk individuals for different diseases from their genotypes. However, the broader application of PRS to the general population is hindered by the limited transferability of PRS developed in Europeans to non-European populations. To improve PRS prediction accuracy in non-European populations, we develop a statistical method called SDPRX that can effectively integrate genome wide association study summary statistics from different populations. SDPRX automatically adjusts for linkage disequilibrium differences between populations and characterizes the joint distribution of the effect sizes of a variant in two populations to be both null, population specific, or shared with correlation. Through simulations and applications to real traits, we show that SDPRX improves the prediction performance over existing methods in non-European populations.

Introduction

The polygenic risk score (PRS) of a complex trait for a given individual is constructed by combining the estimated effect sizes of genetic markers across the genome for this individual. PRS has received great interest recently because of its ability to identify individuals with high disease risk for more effective population screening, diagnosis, and monitoring.[1] However, PRSs for most diseases to date have been primarily developed for Europeans, as most well-powered genome-wide association studies (GWASs) have been performed in cohorts of European ancestry. There can be substantial reduction in prediction accuracy when the PRSs derived from European samples are directly applied to non-European populations, leading to possible health disparities.[2,3]

The limited generalizability of PRS across different populations may be attributed but not limited to a number of factors. First, there is a lack of well-powered GWASs for training PRS models in the non-European populations. Second, the pattern of linkage disequilibrium (LD) and the tagging of causal variants can be different across populations. Third, the allele frequencies of variants vary between populations, and some variants can even be population specific. As a general rule, the effect sizes of rarer variants are harder to estimate and GWASs with larger sample size are required in order to provide accurate estimates. Fourth, the effect sizes of one variant can be null (i.e., no effect), population specific (non-zero in one population), or correlated in two populations.[4,5] Therefore, the effect sizes estimated from European GWASs may or may not be directly transferable to other populations.

Great efforts have been made in recent years to improve the genetic diversity of GWASs.[6,7] Increased availability of GWAS summary statistics and biobank data from non-European ancestries creates an opportunity for developing novel methods to improve the accuracy of PRS in different populations. One general approach is to first estimate effect sizes in each population separately and then derive a linear combination of the estimated effect sizes from a validation dataset of the target population.[8] Other approaches include jointly modeling GWAS summary statistics from multiple populations under the assumption that the causal variants are largely shared across populations.[9–12]

Here, we propose SDPRX, an extension of SDPR,[13] which integrates GWAS summary statistics and LD matrices from two populations with effect sizes under a hierarchical Bayesian model. SDPRX characterizes the joint distribution of the effect sizes of a SNP (single-nucleotide polymorphism) in two populations to be both null, population specific, or shared with correlation. We compared the performance of SDPRX with existing methods through extensive simulations and applications to 15 traits in the East Asian (EAS) and seven traits in the African (AFR) individuals from the UK Biobank.[14] We show that SDPRX may substantially improve the prediction accuracy in non-European populations over the existing methods.

Material and methods

Overview of SDPRX

As a hierarchical Bayesian model, SDPRX has two parts—likelihood and prior (Figure 1). The likelihood connects the pair of marginal effect sizes in GWAS summary statistics from the two populations with true effect sizes through a multivariate normal distribution accounting for LD:

$$\widehat{\beta}_1 \mid \eta, \, \beta_1 \sim N(\boldsymbol{R}_1 \, \eta\beta_1, \, \boldsymbol{R}_1/N_1 + a\boldsymbol{I})$$
$$\widehat{\beta}_2 \mid \eta, \, \beta_2 \sim N(\boldsymbol{R}_2 \, \eta\beta_2, \, \boldsymbol{R}_2/N_2 + a\boldsymbol{I}) \quad , \qquad \text{(Equation 1)}$$

[1]Program in Computational Biology and Bioinformatics, Yale University, New Haven, CT, USA; [2]Department of Biostatistics, Yale School of Public Health, New Haven, CT, USA
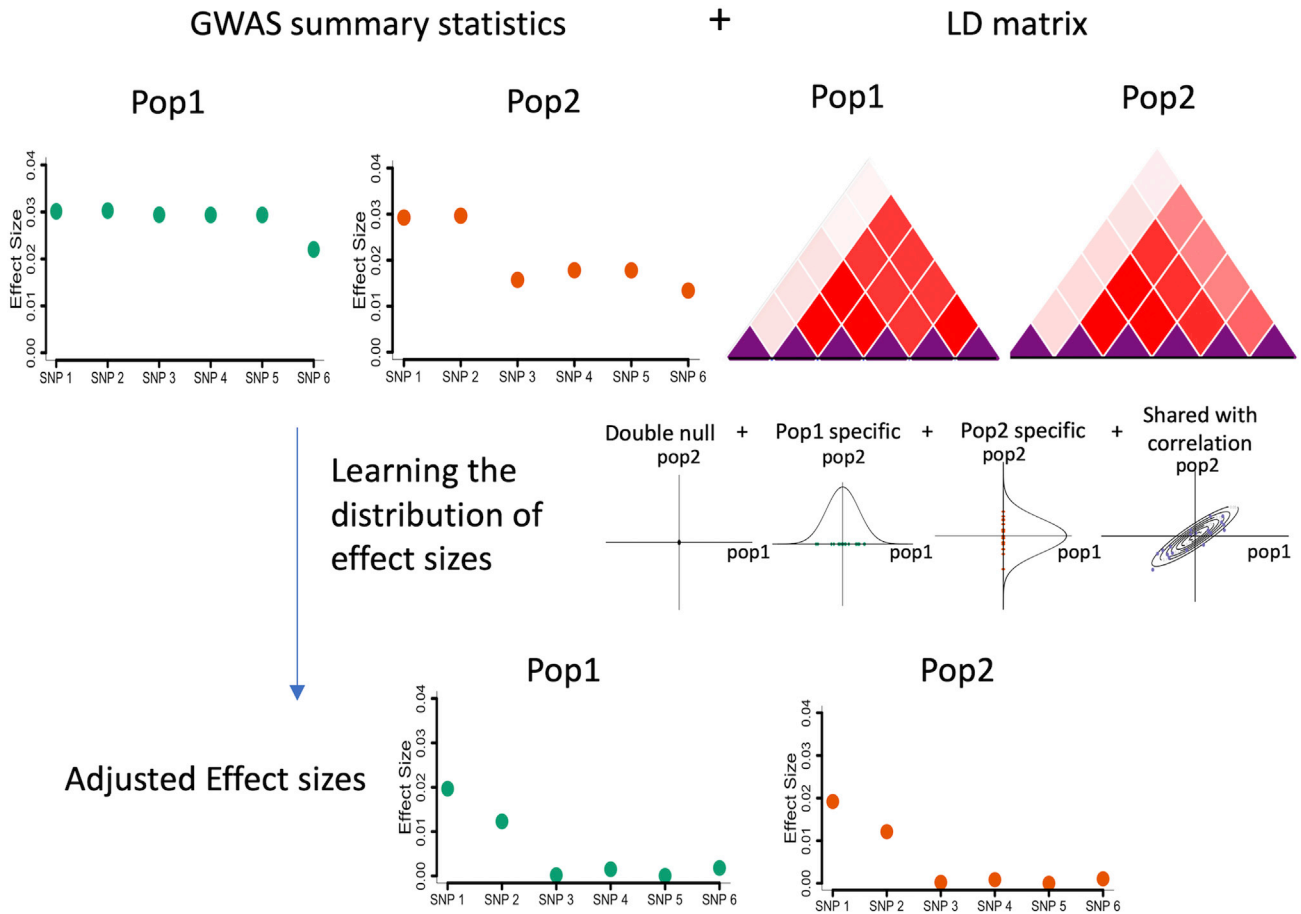*Correspondence: hongyu.zhao@yale.edu

Figure 1. Illustration of the modeling framework of SDPRX
SDPRX integrates GWAS summary statistics and LD matrices from two populations through the likelihood function. The prior characterizes the joint distribution of the effect sizes of a SNP in two populations to be both null, population specific, or shared with correlation. After fitting the model through MCMC, it outputs the adjusted effect sizes for calculation of PRS.

where $\widehat{\boldsymbol{\beta}}_1$ and $\widehat{\boldsymbol{\beta}}_2$ are the marginal effect sizes, $\boldsymbol{R}_1$ and $\boldsymbol{R}_2$ are the LD matrices, and N_1 and N_2 are GWAS sample sizes for populations 1 and 2, respectively. Compared with the commonly used assumption $\widehat{\boldsymbol{\beta}}|\boldsymbol{\beta} \sim N(\boldsymbol{R}\boldsymbol{\beta}, \boldsymbol{R}/N)$, the function above has two variations.[13] First, it shrinks the off-diagonal covariance by a constant identity matrix aI to avoid the over-estimation of effect sizes β_1 and β_2 for SNPs in high LD as a result of the mismatch between GWAS summary statistics and reference panel. Second, it introduces a redundant parameter η so that the choice of hyperparameters of the prior on the variance components does not constrain the posterior inference.[15] We set $N_1a = N_2a = 1$ and let $\eta \sim N(0, 10^6)$ based on our SDPR paper as a small shrinkage would allow the algorithm to converge.[13]

For each SNP j, we then specify the following joint distribution as the prior on the effect sizes (β_{j1}, β_{j2}) in two populations

$$
\begin{pmatrix} \beta_{j1} \\ \beta_{j2} \end{pmatrix} \sim p_0 \begin{pmatrix} \delta_0 \\ \delta_0 \end{pmatrix} + p_1 \sum_{k=1}^{1000} \pi_{1k} \begin{pmatrix} N(0, \sigma_{1k}^2) \\ \delta_0 \end{pmatrix} +
$$
$$
p_2 \sum_{k=1}^{1000} \pi_{2k} \begin{pmatrix} \delta_0 \\ N(0, \sigma_{2k}^2) \end{pmatrix} +
$$
$$
p_3 \sum_{k=1}^{1000} \pi_{3k} N\left(\begin{pmatrix} 0 \\ 0 \end{pmatrix}, \sigma_{3k}^2 \begin{pmatrix} 1 & \rho \\ \rho & 1 \end{pmatrix} \right)
$$

$(\text{Equation } 2)$

This prior characterizes the genetic architecture of one trait in two populations by a mixture of four mutually exclusive components. The first term describes the effect sizes of one SNP as zero (Dirichlet delta distribution) in both populations. The second, third, and fourth terms represent the effect sizes of one SNP as non-zero in population 1 only, non-zero in population 2 only, or non-zero and correlated in both populations. We note that if a SNP is only present in one population, it will be assigned to the first term (null) or one of the second and third terms (population specific).

We further assigned a Dirichlet distribution prior on the probability of each SNP to be null (p_0), population 1 specific (p_1), population 2 specific (p_2), and shared with correlation (p_3).

$$(p_0, p_1, p_2, p_3) \sim Dir(1) \qquad (\text{Equation } 3)$$

In simulation and real data analysis, we often found that SDPRX over-estimated the proportion of SNPs with population-specific effects and under-estimated the proportion of SNPs with shared effects, which was due to the identifiability issues caused by SNPs in high LD (Figure S1). To fix this issue, we introduce an option for SDPRX assuming no population-specific effects for shared variants ($p_0 = 0.25, p_1 = p_2 = 0, p_3 = 0.25$). We found that this option improved the prediction accuracy for most traits in real data analysis, suggesting that the genetic effects for most complex traits are indeed shared

across ancestries. We recommend the user to run both options and select the better result based on the validation dataset.

SDPRX adopts the idea of Bayesian nonparametric prior from SDPR, which is adaptive to different parametric assumptions. Specifically, for the second (population 1 specific), third (population 2 specific), and fourth terms (shared with correlation), we used the truncated stick-breaking process to represent the variance components and probability of assignments.[16] The truncation needs to be applied so that the maximum number of components of the mixture model is finite. We found that setting the maximum components to 1,000 was sufficient for our simulation and real data application because the number of non-trivial components, to which SNPs were assigned, was way fewer than 1,000. For example, for the second term (population 1 specific), we had:

$$V_{1k} \sim Beta(1, \alpha_1), \ k = 1, \dots, 1000$$

$$\pi_{11} = V_{11}$$

$$\pi_{1k} = \prod_{m=1}^{k-1}(1 - V_{1m})V_{1k}, \ k = 2, \dots 1000$$

$$\sigma_{1k}^2 \sim IG(.5, .5)$$

$$\alpha_1 \sim Gamma(0.1, 0.1). \qquad \text{(Equation 4)}$$

The cross-population genetic correlation ρ can be obtained from software like Popcorn.[17] We set rho to the estimated value in simulation and real data analysis. To reduce the computational burden, SDPRX partitioned the LD matrix (element-wise maximum of LD matrices from two populations) into approximately independent LD blocks.[13,18] We developed a Markov chain Monte Carlo (MCMC) algorithm based on the Gibbs sampler to fit the model (supplemental methods). In practice, we used 1,000 MCMC iterations and the first 200 iterations as the burn-in. We outputted the mean posterior effect sizes $\eta\beta_1$ and $\eta\beta_2$ as the weights to derive PRS for two populations. When an independent validation dataset is available, one can also perform a convex combination of the output weights (α increased from 0 to 1 by a step of 0.05) and select the best α to further optimize the performance:

$$\beta_{target} = \alpha\beta_1 + (1 - \alpha)\beta_2. \qquad \text{(Equation 5)}$$

Existing methods

We compared the performance of SDPRX with five other methods: (1) PRS-CSx as implemented in the PRS-CSx software; (2) LDpred2 as implemented in the bigsnpr package; (3) XPASS as implemented in the XPASS package; (4) DBSLMM as implemented in the DBSLMM package; and (5) Lassosum as implemented in the Lassosum package. For PRS-CSx, the global shrinkage parameter was specified as {1e−6, 1e−4, 1e−2, 1, auto}. For LDpred2, we ran LDpred2-inf, LDpred2-auto, and LDpred2-grid and reported the best performance of three options. The grid of hyperparameters was set as non-sparse, p in a sequence of 21 values from 10^{-5} to 1 on a log-scale, and h^2 within {0.7, 1, 1.4} of h^2_{LDSC}. For XPASS, population-specific effects were included in both populations (p $< 10^{-10}$, clump_r^2 = 0.1, clump_kb = 1,000). For DBSLMM, p value threshold was iterated within {10^{-5}, 10^{-6}, 10^{-7}, 10^{-8}}, r^2 was iterated within {0.05, 0.1, 0.15, 0.2, 0.25}, and h^2 was set as h^2_{LDSC}. For Lassosum, lambda was set in a sequence of 20 values from 0.001 to 0.1 on a log-scale and s

within {0.2, 0.5, 0.9, 1}. In real data analysis, we also performed a linear regression of phenotype on the PRS of two populations on the validation dataset to learn the weights for combination of effect sizes.

Simulations

To simulate individual-level genotypes from the 1000 Genomes Phase 3 haplotype, we first randomly selected 3,000 SNPs from the first 30,000 common SNPs (minor allele frequency [MAF] > 0.05 in East Asians (EAS), Europeans (EUR), and Africans (AFR)) on chromosomes 1 to 10. The curated haplotypes reduced the computational burden of Hapgen2 while still providing a good representation of the real population structure. The simulated genotypes all passed the quality control (MAF > 0.05, genotype missing rate < 0.1, p value of Hardy-Weinberg Equilibrium test (pHWE) $> 10^{-6}$).

We generated the simulated effect sizes of SNPs for two populations (EUR + EAS or EUR + AFR) according to the following model:

$$\begin{pmatrix} \beta_{j1} \\ \beta_{j2} \end{pmatrix} \sim (1 - p_1 - p_2 - p_3)\begin{pmatrix} \delta_0 \\ \delta_0 \end{pmatrix} + p_1\begin{pmatrix} N\left(0, \frac{0.2h^2}{Mp_1}\right) \\ \delta_0 \end{pmatrix} +$$

$$p_2\begin{pmatrix} \delta_0 \\ N\left(0, \frac{0.2h^2}{Mp_2}\right) \end{pmatrix} +$$

$$p_3\, N\left(\begin{pmatrix} 0 \\ 0 \end{pmatrix}, \frac{0.8h^2}{Mp_3}\begin{pmatrix} 1 & \rho \\ \rho & 1 \end{pmatrix}\right),$$

where $h^2 = 0.3$ and $M = 30,000$. We mainly considered four scenarios by increasing the proportions of population-specific and shared causal variates: (1) $p_1 = p_2 = p_3 = 0.0005$, (2) $p_1 = p_2 = p_3 = 0.005$, (3) $p_1 = p_2 = p_3 = 0.05$, and (4) $p_1 = p_2 = 0.05, p_3 = 0.9$. We also varied the cross-population genetic correlation ρ in {0.4, 0.6, 0.8}. Additionally, we considered one simulation setting based on scenario 3 to evaluate the performance of each method on admixed individuals. We then generated phenotypes from simulated effect sizes by using GCTA-sim, and we performed marginal linear regression analysis on the training data to obtain summary statistics by using PLINK2.[19,20]

UK Biobank analysis

We downloaded GWAS summary statistics from GIANT, DIAGRAM, GLGC, BBJ, and PAGE consortia.[6,7,21–26] We followed the guideline of LDHub to perform quality control on the GWAS summary statistics for each population.[27] We removed strand-ambiguous (A/T and G/C) SNPs, insertions and deletions (INDELs), and SNPs with an effective sample size less than 0.67 times the 90th percentile of sample size. We did not restrict to SNPs present in two GWAS summary statistics so that population-specific SNPs would be retained. Table 1 shows the number of SNPs present in the summary statistics for each trait after intersecting with reference panel and test dataset. The number of SNPs may not be optimal to achieve the best performance for each trait, but it did allow a fair comparison of different methods. We used the 1000 Genomes EUR, EAS, and AFR samples as the LD reference panel for EUR, EAS, and AFR (admixed populations for PAGE study) summary statistics, respectively. For UK Biobank, we first performed principal-component analysis (PCA) together with 1000 Genomes samples. We then trained a random forest classifier to assign UK Biobank samples to one of five super populations (EUR, EAS, AFR, South Asians [SAS], Admixed Americans [AMR]) on the basis of the top ten PCs (Figure S2). We retained 2,091

Table 1. Summary of sample size and SNPs in GWAS summary statistics and UK Biobank datasets

	GWAS sample size (EUR/EAS/AFR)	1KG HM3 and GWAS and UKB SNPs (EAS)	1KG HM3 and GWAS and UKB SNPs (AFR)	UKB EAS sample size (EAS)	UKB AFR sample size (AFR)
Height	252,230[21]/159,095[26]/49,781[6]	775,077	753,371	2,081	6,727
BMI	233,766[22]/158,284[25]/49,335[6]	755,775	832,542	2,078	6,715
HDL	885,540[7]/116,404[7]/90,804[7]	711,038	832,494	398	1,610
LDL	840,006[7]/79,693[7]/87,559[7]	772,482	832,494	440	1,710
Total cholesterol	929,732[7]/144,579[7]/92,554[7]	445,763	832,494	440	1,714
Triglycerides	860,547[7]/81,071[7]/89,467[7]	772,505	832,494	440	1,714
Eosinophils	563,085[28]/62,076[29]/N/A	757,167	N/A	2,026	N/A
Lymphocytes	563,085[28]/62,076[29]/N/A	757,167	N/A	2,026	N/A
Monocytes	563,085[28]/62,076[29]/N/A	757,167	N/A	2,026	N/A
Neutrophils	563,085[28]/62,076[29]/N/A	757,167	N/A	2,026	N/A
Red blood cells	563,085[28]/108,794[29]/N/A	757,167	N/A	2,028	N/A
White blood cells	563,085[28]/107,964[29]/N/A	757,167	N/A	2,028	N/A
Platelets	563,085[28]/108,208[29]/N/A	757,167	N/A	2,028	N/A
Coronary artery disease	61,294[30]/101,091[31]/N/A	761,770	N/A	1,116	N/A
Type 2 diabetes	156,109[23]/191,764[24]/14,480[6]	570,266	722,296	1,263	4,809

The union of SNPs in GWAS summary statistics of two populations passing the quality control were intersected with the 1000 Genomes Hapmap3 reference panel and UK Biobank to form the final SNP list.

unrelated EAS and 6,829 unrelated AFR samples with a predicted probability greater than 0.9 to form the validation and test datasets. We also selected 410 self-reported Black admixed individuals from UK Biobank, as we found that the random forest classifier was not able to accurately identify admixed individuals. We obtained a total of around 800K Hapmap3 (HM3) SNPs after intersecting with the SNPs of summary statistics and reference panel.

Phenotypes were selected on the basis of the relevant data fields (50 for height, 21001 for BMI, 30780 for low-density lipoprotein [LDL], 20760 for high-density lipoprotein [HDL], 20690 for total cholesterol [TC], 30870 for triglycerides [TG], 30150 for count of eosinophil [EOS], 30120 for lymphocyte [LYM], 30130 for monocyte [MON], 30140 for neutrophil [NEU], 30010 for red blood cell [RBC], 30000 for white blood cell [WBC], 30080 for platelet [PLT], and self-report questionnaire and in-hospital record for coronary artery disease [CAD] and type 2 diabetes). For 13 quantitative traits, we reported the prediction R^2 of PRS (variance explained by PRS) defined as $R^2 = 1 - \frac{SS1}{SS0}$, where $SS0$ is the sum of squares of the residuals of the restricted linear regression model with covariates (an intercept, age, sex, top ten PCs of the genotype data) and $SS1$ is the sum of squares of the residuals of the full linear regression model (covariates above and PRS). For two binary traits, we reported the area under the curve (AUC) of PRS only for better comparison of different methods. The percentage of the improvement of method A over method B was defined as $(metric_A - metric_B)/metric_B$.

Results

Simulations

We first evaluated the prediction performance of each method via simulations across different genetic architectures and training sample sizes. We focused on six methods—SDPRX, PRS-CSx,[10] LDpred2,[32] XPASS,[9] DBSLMM,[33] and Lassosum.[34] LDpred2, DBSLMM, and Lassosum are single population methods that take non-EUR GWAS summary statistics as input, while SDPRX, PRS-CSx, and XPASS are multi-discovery methods that jointly integrate GWAS summary statistics from multiple populations. We used Hapgen2 to simulate individual-level genotypes of European (EUR), East Asian (EAS), and African (AFR) populations by using the 1000 Genomes Phase 3 as the reference haplotypes.[35,36] We also used admix-simu to simulate admixed individuals by a model of one pulse of admixture nine generations ago with 80% contribution from AFR and 20% from EUR.[37] Due to computational constraints, we only included 30,000 SNPs in total by selecting 3,000 SNPs from each of chromosomes 1 to 10. The training cohort consisted of 40K EUR individuals and varying sample sizes (10, 20, 40K) of EAS and AFR individuals. The reduced sample size of non-EUR populations aligns with the fact that the sample size of most non-EUR GWASs is smaller than EUR GWASs. The validation and test datasets consisted of 5K individuals of each population. The genetic architecture was simulated for two populations (EUR + EAS or EUR + AFR) as follows. Effect sizes of one SNP in two populations can be both zero, population specific (non-zero in population 1 or population 2), or correlated with the cross-population genetic correlation. We fixed the total heritability to be 0.3 and assumed that 80% of the total heritability was explained by SNPs with correlated effect sizes between the two populations (material and methods). The proportion of SNPs with population 1-specific, population 2-specific, and correlated effect sizes was equally set to be

0.05% (scenario 1), 0.5% (scenario 2), and 5% (scenario 3). For scenario 4, the proportion of SNPs with population 1-specific and population 2-specific effect sizes were set to 5% and the proportion of SNPs with shared effect sizes was set to 90%. The cross-population genetic correlation was set to be 0.8 (Figure 2), 0.6 (Figure S3), and 0.4 (Figure S4). Each simulation setting was repeated 10 times. Further details of simulation can be found in the material and methods section.

We generated summary statistics via regression analysis of the training cohort as the input to SDPRX, PRS-CSx,[10] LDpred2,[32] XPASS,[9] DBSLMM,[33] and Lassosum.[34] We used the validation dataset to estimate LD matrix for each method and tune parameters for LDpred2, PRS-CSx, DBSLMM, and Lassosum. The prediction performance was assessed by the square of Pearson correlation of PRS and simulated phenotype in the independent test dataset. We mainly focused on the results in EAS and AFR because our main purpose is to jointly utilize EUR GWAS data to improve the performance of PRS in non-EUR populations.

Overall, all methods performed better as the proportion of causal SNPs decreased (Figure 2 and Table S1). Under a highly sparse genetic architecture (scenario 1), the increase of sample size provided minimal benefits because the effect size per causal SNP was large enough for accurate estimation. In contrast, the improvement with an increasing sample size became apparent when the genetic architecture was polygenic (scenarios 3 and 4). Among all methods, XPASS did not perform well in the sparse setting as the simulated data violated its assumption that all SNPs are causal. LDpred2 had descent accuracy when the genetic architecture was sparse or the sample size was large. However, there was clear advantage of cross-population methods (SDPRX and PRS-CSx) over LDpred2 when the genetic architecture was polygenic (scenarios 3 and 4) and the sample size was small (10 and 20K). Results were similar for lower genetic correlations (Figures S3 and S4; Tables S2 and S3) and admixed population (Figure S5). These results suggest that jointly modeling EUR and non-EUR GWASs can improve the prediction accuracy in non-EUR populations if non-EUR GWAS alone was not well powered. We can see that SDPRX outperformed the other methods in most cases.

Prediction performance for UK Biobank traits
We next compared the performance of SDPRX with other methods in predicting 13 quantitative traits (height, body mass index, high-density lipoproteins, low-density lipoproteins, total cholesterol, triglycerides, count of eosinophil, lymphocyte, monocyte, neutrophil, red blood cell, white blood cell and platelet) and two binary traits (type 2 diabetes and coronary artery disease) for EAS individuals in UK Biobank. For AFR individuals, the performance was compared with six quantitative traits and one binary trait because of the limited number of publicly available summary statistics. For AMR individuals, the comparison was limited to height and BMI, as fewer than 100 individuals

had records for other traits in UK Biobank. We obtained public GWAS summary statistics and performed quality control to standardize the input (details in material and methods; Table 1). Individuals in the GWAS do not overlap with individuals in UK Biobank. EUR, EAS, and AFR samples from the 1000 Genomes Project were used to construct the reference LD matrix for each method. We selected unrelated EAS and AFR individuals in UK Biobank on the basis of a random forest classifier (Figure S2). AMR individuals were selected on the basis of self-reported questionnaire. For each population, we randomly assigned 1/3 of participants to the validation dataset for parameter tuning and learning the linear combination of effect sizes. The remaining participants formed the test dataset for evaluation of the prediction performance. The random assignment was repeated for 20 times. We reported the prediction R^2 of PRS (variance explained by PRS) for 13 quantitative traits and the AUC of PRS for two binary traits.

We first investigated the prediction accuracy of each method in EAS (Figure 3 and Table S4) without learning the linear combination of effect sizes. Consistent with simulations, SDPRX achieved the highest prediction accuracy in all traits. The average improvement of SDPRX was 67% over LDpred2, 40% over DBSLMM, and 86% over Lassosum, suggesting that jointly modeling EUR and EAS GWAS summary statistics indeed provided benefits compared with using EAS GWAS summary statistics alone. SDPRX was also on average 23% and 56% better than PRS-CSX and XPASS. We then linearly combined EUR and EAS effect sizes for each method by weights learned on the validation dataset. SDPRX remained the best method for ten traits with an average 11%, 28%, 19%, 17%, and 43% improvement over PRS-CSX, LDpred2, XPASS, DBSLMM, and Lassosum (Figure S6 and Table S5), respectively.

Results for AFR were similar to results for EAS (Figure 4 and Table S6). SDPRX performed best in most traits regardless of learning the linear combination of effect sizes. The average improvement of SDPRX over PRS-CSx, LDpred2, XPASS, DBSLMM, and Lassosum was 27%, 12%, 44%, 38%, and 51% before the linear combination and 17%, 36%, 37%, 24%, and 42% after the linear combination (Figure S7 and Table S7). We also evaluated the performance of each method for height and BMI for the limited number of AMR individuals in UK Biobank and found that SDPRX outperformed the other methods as well (Figure S8).

Discussion

SDPRX takes GWAS summary statistics from two populations as input and thus is able to leverage shared information from two populations to better estimate the effect sizes of SNPs compared with single population methods such as LDpred2. The prior assumption made by SDPRX is more general than XPASS and PRS-CSx. Unlike SDPRX, XPASS assumes that the genetic architecture is polygenic
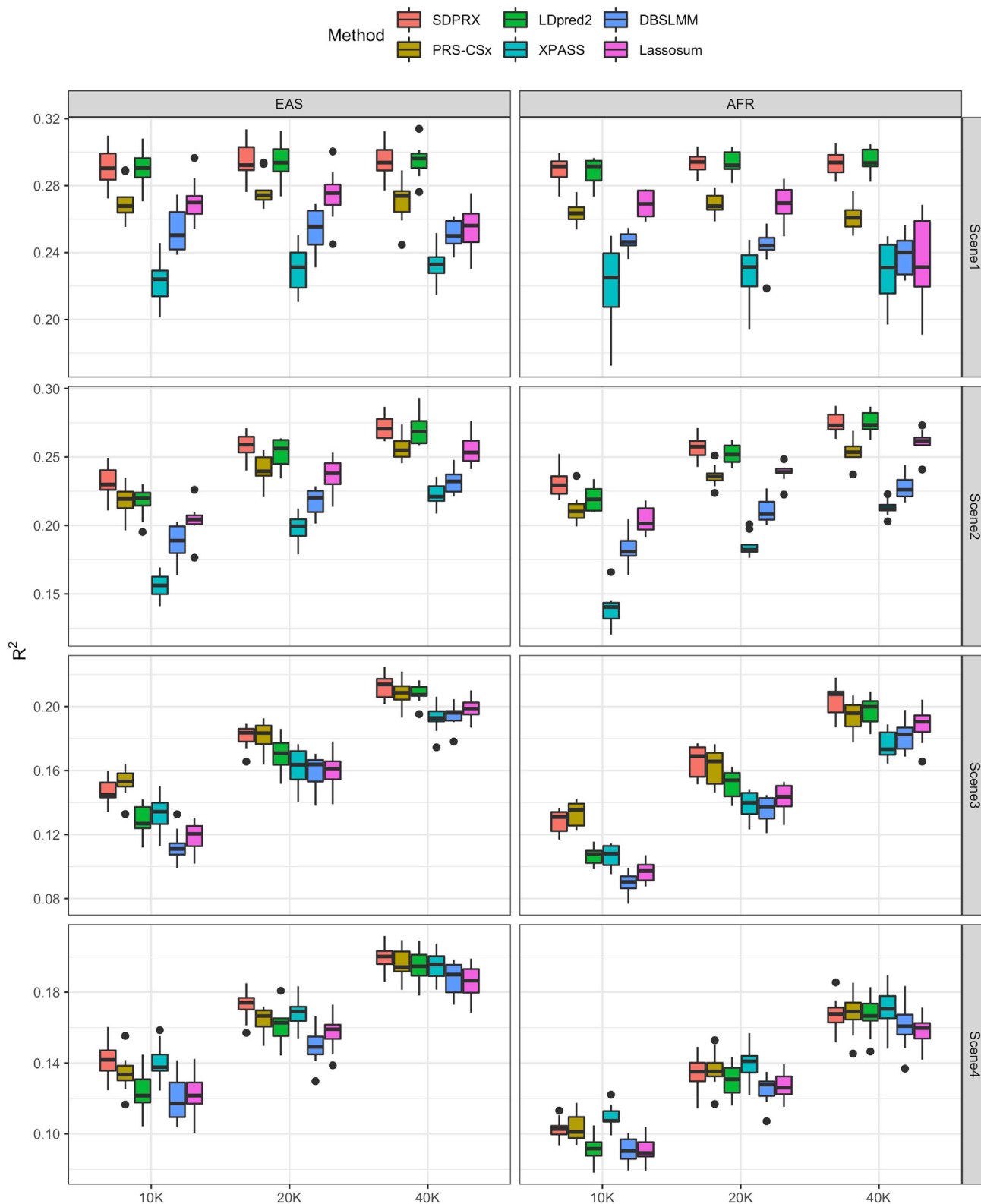
Figure 2. Prediction performance of different methods on simulated data
The proportion of SNPs with population 1-specific, population 2-specific, and correlated effect sizes was equally set to be 0.05% (scenario 1), 0.5% (scenario 2), and 5% (scenario 3). For scenario 4, the proportion of SNPs with population 1-specific and population 2-specific effect sizes were set to 5% and the proportion of SNPs with shared effect sizes was set to 90%. The cross-population genetic correlation was set to 0.8 and the heritability was 0.3. Simulation in each scenario was repeated for 10 times. For each boxplot, the central mark is the median and the lower and upper edges represent the 25th and 75th percentiles.
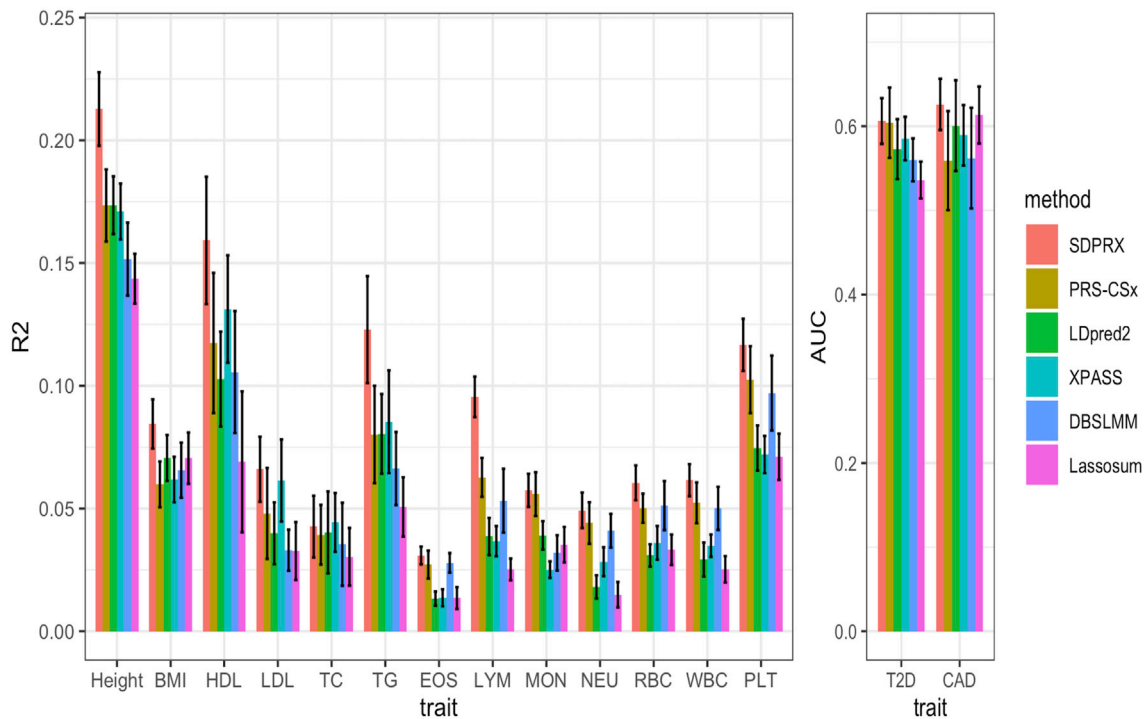
Figure 3. Prediction performance of different methods for 13 quantitative traits and two binary traits in EAS samples from UK Biobank without the linear combination of effect sizes

Selected participants with corresponding phenotypes were randomly split to form the validation (1/3) and test datasets (2/3). The mean and standard deviation of R^2 (quantitative trait) and AUC (binary trait) across 20 random splits are showed on the bar plot.

and all SNPs have non-zero effect sizes while empirically methods assuming only part of SNPs having non-zero effect sizes often have better performance. Compared with PRS-CSx, SDPRX directly incorporates the cross-population genetic correlation into the model for better estimation of shared effect sizes. These points, taken together, may explain why SDPRX outperformed the other methods in both simulation and real data analyses.

Although SDPRX improves the prediction accuracy in non-EUR populations, it is far from overcoming the gap between performance of PRS in EUR and non-EUR populations. We think developing computational methods alone will not be able to solve this issue, and there are two points that may explain the gap based on the results presented in this paper. First, the sample sizes of non-EUR GWASs are limited. Results in EAS were overall better than results in AFR because of the larger sample size of EAS GWASs. Second, other factors such as genetic architecture may be different for some traits in two populations. For example, the performance of HDL, LDL, TC, and TG was different in EAS and AFR in spite of similar GWAS sample sizes. We also note that social, environmental, and familial factors were not considered in this study because we primarily focused on comparison of methods, though they may play an important role in the transferability of PRS.[3]

The computational time and memory usage of all methods are listed in Table S8. For SDPRX and PRS-CSx, we paralleled computation over 22 chromosomes and used three threads per chromosome for the linear algebra library ($22 \times 3 = 66$ threads in total). The time and memory usage are reported for the longest chromosome, which was the rate-limiting step. LDpred2 was run in the genome-wide mode with ten threads for parallel computation. DBSLMM and Lassosum were run with three threads for parallel computation. No parallelization was used for XPASS. One should keep in mind that the number of MCMC iterations and threads for parallel computation affects the computation time significantly, though we did not explore it in this paper. Overall, the methods that do not need to perform MCMC (XPASS, DBSLMM, and Lassosum) were faster than the methods that need to perform MCMC (SDPRX, PRS-CSx, and LDpred2). SDPRX was able to finish the job in 10 h without consuming a large amount of memory.

Lastly, we note three limitations of our current work that we will address in the future. First, similar to other studies (e.g., PRS-CSx), we restricted to HM3 SNPs for an easy comparison of different methods, which is not optimal, as it might not include some informative SNPs. Second, SDPRX is currently not designed for admixed populations, which is challenging as the LD pattern would be heterogenous and difficult to capture with a single LD matrix. To our knowledge, how to connect the marginal effect sizes in the GWAS summary statistics derived from admixed populations with true effect sizes is also less clear, which may deal with the adjustment of local ancestry and covariates.[38,39] Third, methods utilizing functional annotation have shown to improve the performance in both single
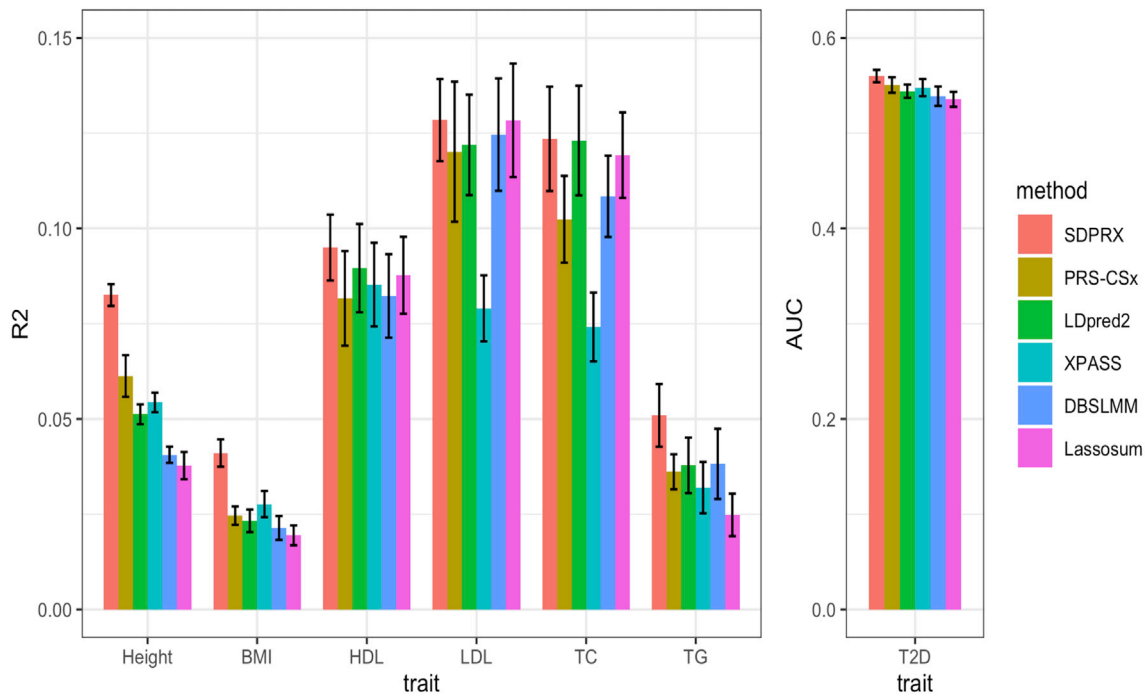
Figure 4. Prediction performance of different methods for six quantitative traits and one binary trait in AFR samples from UK Biobank without the linear combination of effect sizes
Selected participants with corresponding phenotypes were randomly split to form the validation (1/3) and test datasets (2/3). The mean and standard deviation of R^2 (quantitative trait) and AUC (binary trait) across 20 random splits are showed on the bar plot.

and cross-population settings.[40,41] Incorporating functional annotation may further improve the performance of SDPRX.

Data and code availability

SDPRX is available at https://github.com/eldronzhou/SDPRX. The code used in this paper is available at https://github.com/eldronzhou/SDPRX_paper. The links to summary statistics can be found in the web resources.

Supplemental information

Supplemental information can be found online at https://doi.org/10.1016/j.ajhg.2022.11.007.

Acknowledgments

Declaration of interests

The authors declare no competing interests.

Web resources

Admix-simu, https://github.com/williamslab/admix-simu
BBJ summary statistics, http://jenger.riken.jp/en/result
BCX summary statistics, ftp://ftp.sanger.ac.uk/pub/project/humgen/summary_statistics/UKBB_blood_cell_traits/
CARDIoGRAMplusC4D summary statistics, http://www.cardiogramplusc4d.org/data-downloads/
DIAGRAM summary statistics, https://diagram-consortium.org/downloads.html
GIANT summary statistics, https://portals.broadinstitute.org/collaboration/giant/index.php/GIANT_consortium_data_files-GIANT_Consortium_2012-2015_GWAS_Summary_Statistics
GLGC summary statistics, http://csg.sph.umich.edu/willer/public/glgc-lipids2021/results/ancestry_specific/
LDpred2, https://github.com/privefl/bigsnpr
PAGE summary statistics, https://www.ebi.ac.uk/gwas/studies/GCST008053
PLINK, https://www.cog-genomics.org/plink/
Popcorn, https://github.com/brielin/Popcorn
PRS-CSx, https://github.com/getian107/PRScsx
XPASS, https://github.com/YangLabHKUST/XPASS

References

1. Khera, A.V., Chaffin, M., Aragam, K.G., Haas, M.E., Roselli, C., Choi, S.H., Natarajan, P., Lander, E.S., Lubitz, S.A., Ellinor, P.T., and Kathiresan, S. (2018). Genome-wide polygenic scores for

common diseases identify individuals with risk equivalent to monogenic mutations. Nat. Genet. *50*, 1219–1224.

2. Duncan, L., Shen, H., Gelaye, B., Meijsen, J., Ressler, K., Feldman, M., Peterson, R., and Domingue, B. (2019). Analysis of polygenic risk score usage and performance in diverse human populations. Nat. Commun. *10*, 3328.

3. Martin, A.R., Kanai, M., Kamatani, Y., Okada, Y., Neale, B.M., and Daly, M.J. (2019). Clinical use of current polygenic risk scores may exacerbate health disparities. Nat. Genet. *51*, 584–591.

4. Shi, H., Gazal, S., Kanai, M., Koch, E.M., Schoech, A.P., Siewert, K.M., Kim, S.S., Luo, Y., Amariuta, T., Huang, H., et al. (2021). Population-specific causal disease effect sizes in functionally important regions impacted by selection. Nat. Commun. *12*, 1098.

5. Shi, H., Burch, K.S., Johnson, R., Freund, M.K., Kichaev, G., Mancuso, N., Manuel, A.M., Dong, N., and Pasaniuc, B. (2020). Localizing components of shared transethnic genetic architecture of complex traits from GWAS summary data. Am. J. Hum. Genet. *106*, 805–817.

6. Wojcik, G.L., Graff, M., Nishimura, K.K., Tao, R., Haessler, J., Gignoux, C.R., Highland, H.M., Patel, Y.M., Sorokin, E.P., Avery, C.L., et al. (2019). Genetic analyses of diverse populations improves discovery for complex traits. Nature *570*, 514–518.

7. Graham, S.E., Clarke, S.L., Wu, K.H.H., Kanoni, S., Zajac, G.J.M., Ramdas, S., Surakka, I., Ntalla, I., Vedantam, S., Winkler, T.W., et al. (2021). The power of genetic diversity in genome-wide association studies of lipids. Nature *600*, 675–679.

8. Weissbrod, O., Kanai, M., Shi, H., Gazal, S., Peyrot, W., Khera, A., Okada, Y., Martin, A., Finucane, H., and Price, A.L. (2021). Leveraging fine-mapping and non-European training data to improve trans-ethnic polygenic risk scores. Preprint at medRxiv. https://doi.org/10.1101/2021.01.19.21249483.

9. Cai, M., Xiao, J., Zhang, S., Wan, X., Zhao, H., Chen, G., and Yang, C. (2021). A unified framework for cross-population trait prediction by leveraging the genetic correlation of polygenic traits. Am. J. Hum. Genet. *108*, 632–655.

10. Ruan, Y., Anne Feng, Y.-C., Chen, C.-Y., Lam, M., Sawa, A., Martin, A.R., Qin, S., Huang, H., and Ge, T. (2021). Improving polygenic prediction in ancestrally diverse populations. Preprint at medRxiv. https://doi.org/10.1101/2020.12.27.20248738.

11. Spence, J.P., Sinnott-Armstrong, N., Assimes, T.L., and Pritchard, J.K. (2022). A flexible modeling and inference framework for estimating variant effect sizes from GWAS summary statistics. Preprint at bioRxiv. https://doi.org/10.1101/2022.04.18.488696.

12. Zhang, H., Zhan, J., Jin, J., Zhang, J., Ahearn, T.U., Yu, Z., O'Connell, J., Jiang, Y., Chen, T., Team, a.R., et al. (2022). Novel methods for multi-ancestry polygenic prediction and their evaluations in 3.7 million individuals of diverse ancestry. Preprint at bioRxiv. https://doi.org/10.1101/2022.03.24.485519.

13. Zhou, G., and Zhao, H. (2021). A fast and robust Bayesian nonparametric method for prediction of complex traits using summary statistics. PLoS Genet. *17*, e1009697.

14. Bycroft, C., Freeman, C., Petkova, D., Band, G., Elliott, L.T., Sharp, K., Motyer, A., Vukcevic, D., Delaneau, O., O'Connell, J., et al. (2018). The UK Biobank resource with deep phenotyping and genomic data. Nature *562*, 203–209.

15. Gelman, A. (2006). Prior distributions for variance parameters in hierarchical models (comment on article by Browne and Draper). Bayesian Anal. *1*, 515–534.

16. Ishwaran, H., and James, L.F. (2001). Gibbs Sampling Methods for Stick-Breaking Priors. J. Am. Stat. Assoc. *96*, 161–173.

17. Brown, B.C., Asian Genetic Epidemiology Network Type 2 Diabetes Consortium, Ye, C.J., Price, A.L., and Zaitlen, N. (2016). Transethnic genetic-correlation estimates from summary statistics. Am. J. Hum. Genet. *99*, 76–88.

18. Berisa, T., and Pickrell, J.K. (2016). Approximately independent linkage disequilibrium blocks in human populations. Bioinformatics *32*, 283–285.

19. Yang, J., Lee, S.H., Goddard, M.E., and Visscher, P.M. (2011). GCTA: a tool for genome-wide complex trait analysis. Am. J. Hum. Genet. *88*, 76–82.

20. Chang, C.C., Chow, C.C., Tellier, L.C., Vattikuti, S., Purcell, S.M., and Lee, J.J. (2015). Second-generation PLINK: rising to the challenge of larger and richer datasets. GigaScience *4*, 7.

21. Wood, A.R., Esko, T., Yang, J., Vedantam, S., Pers, T.H., Gustafsson, S., Chu, A.Y., Estrada, K., Luan, J., Kutalik, Z., et al. (2014). Defining the role of common variation in the genomic and biological architecture of adult human height. Nat. Genet. *46*, 1173–1186.

22. Locke, A.E., Kahali, B., Berndt, S.I., Justice, A.E., Pers, T.H., Day, F.R., Powell, C., Vedantam, S., Buchkovich, M.L., Yang, J., et al. (2015). Genetic studies of body mass index yield new insights for obesity biology. Nature *518*, 197–206.

23. Scott, R.A., Scott, L.J., Mägi, R., Marullo, L., Gaulton, K.J., Kaakinen, M., Pervjakova, N., Pers, T.H., Johnson, A.D., Eicher, J.D., et al. (2017). an expanded genome-wide association study of type 2 diabetes in Europeans. Diabetes *66*, 2888–2902.

24. Suzuki, K., Akiyama, M., Ishigaki, K., Kanai, M., Hosoe, J., Shojima, N., Hozawa, A., Kadota, A., Kuriki, K., Naito, M., et al. (2019). Identification of 28 new susceptibility loci for type 2 diabetes in the Japanese population. Nat. Genet. *51*, 379–386.

25. Akiyama, M., Okada, Y., Kanai, M., Takahashi, A., Momozawa, Y., Ikeda, M., Iwata, N., Ikegawa, S., Hirata, M., Matsuda, K., et al. (2017). Genome-wide association study identifies 112 new loci for body mass index in the Japanese population. Nat. Genet. *49*, 1458–1467.

26. Akiyama, M., Ishigaki, K., Sakaue, S., Momozawa, Y., Horikoshi, M., Hirata, M., Matsuda, K., Ikegawa, S., Takahashi, A., Kanai, M., et al. (2019). Characterizing rare and low-frequency height-associated variants in the Japanese population. Nat. Commun. *11*, 1350.

27. Zheng, J., Erzurumluoglu, A.M., Elsworth, B.L., Kemp, J.P., Howe, L., Haycock, P.C., Hemani, G., Tansey, K., Laurin, C.; and Early Genetics and Lifecourse Epidemiology EAGLE Eczema Consortium (2017). LD Hub: a centralized database and web interface to perform LD score regression that maximizes the potential of summary level GWAS data for SNP heritability and genetic correlation analysis. Bioinformatics *33*, 272–279.

28. Vuckovic, D., Bao, E.L., Akbari, P., Lareau, C.A., Mousas, A., Jiang, T., Chen, M.H., Raffield, L.M., Tardaguila, M., Huffman, J.E., et al. (2020). The polygenic and monogenic basis of blood traits and diseases. Cell *182*, 1214–1231.e11.

29. Kanai, M., Akiyama, M., Takahashi, A., Matoba, N., Momozawa, Y., Ikeda, M., Iwata, N., Ikegawa, S., Hirata, M., Matsuda, K., et al. (2018). Genetic analysis of quantitative traits in the Japanese population links cell types to complex human diseases. Nat. Genet. *50*, 390–400.

30. Mehta, N.N. (2011). Large-scale association analysis identifies 13 new susceptibility loci for coronary artery disease. Circ. Cardiovasc. Genet. *4*, 327–329.

31. Koyama, S., Ito, K., Terao, C., Akiyama, M., Horikoshi, M., Momozawa, Y., Matsunaga, H., Ieki, H., Ozaki, K., Onouchi, Y., et al. (2020). Population-specific and trans-ancestry genome-wide analyses identify distinct and shared genetic risk loci for coronary artery disease. Nat. Genet. *52*, 1169–1177.

32. Privé, F., Arbel, J., and Vilhjálmsson, B.J. (2020). LDpred2: better, faster, stronger. Bioinformatics *36*, 5424–5431.

33. Yang, S., and Zhou, X. (2020). Accurate and scalable construction of polygenic scores in large biobank data sets. Am. J. Hum. Genet. *106*, 679–693.

34. Mak, T.S.H., Porsch, R.M., Choi, S.W., Zhou, X., and Sham, P.C. (2017). Polygenic scores via penalized regression on summary statistics. Genet. Epidemiol. *41*, 469–480.

35. 1000 Genomes Project Consortium, Auton, A., Brooks, L.D., Durbin, R.M., Garrison, E.P., Kang, H.M., Korbel, J.O., Marchini, J.L., McCarthy, S., McVean, G.A., and Abecasis, G.R. (2015). A global reference for human genetic variation. Nature *526*, 68–74.

36. Su, Z., Marchini, J., and Donnelly, P. (2011). HAPGEN2: simulation of multiple disease SNPs. Bioinformatics *27*, 2304–2305.

37. Williams, A. (2016). Admix-Simu: Admix-Simu: Program to Simulate Admixture between Multiple Populations (1.0) (Zenodo).

38. Atkinson, E.G., Maihofer, A.X., Kanai, M., Martin, A.R., Karczewski, K.J., Santoro, M.L., Ulirsch, J.C., Kamatani, Y., Okada, Y., Finucane, H.K., et al. (2021). Tractor uses local ancestry to enable the inclusion of admixed individuals in GWAS and to boost power. Nat. Genet. *53*, 195–204.

39. Luo, Y., Li, X., Wang, X., Gazal, S., Mercader, J.M., 23 and Me Research Team; and SIGMA Type 2 Diabetes Consortium, Neale, B.M., Florez, J.C., Auton, A., et al. (2021). Estimating heritability and its enrichment in tissue-specific gene sets in admixed populations. Hum. Mol. Genet. *30*, 1521–1534.

40. Amariuta, T., Ishigaki, K., Sugishita, H., Ohta, T., Koido, M., Dey, K.K., Matsuda, K., Murakami, Y., Price, A.L., Kawakami, E., et al. (2020). Improving the trans-ancestry portability of polygenic risk scores by prioritizing variants in predicted cell-type-specific regulatory elements. Nat. Genet. *52*, 1346–1354.

41. Hu, Y., Lu, Q., Powles, R., Yao, X., Yang, C., Fang, F., Xu, X., and Zhao, H. (2017). Leveraging functional annotations in genetic risk prediction for human complex diseases. PLoS Comput. Biol. *13*, e1005589.

Supplemental information

SDPRX: A statistical method for cross-population prediction of complex traits

Geyu Zhou, Tianqi Chen, and Hongyu Zhao

Supplementary Figures
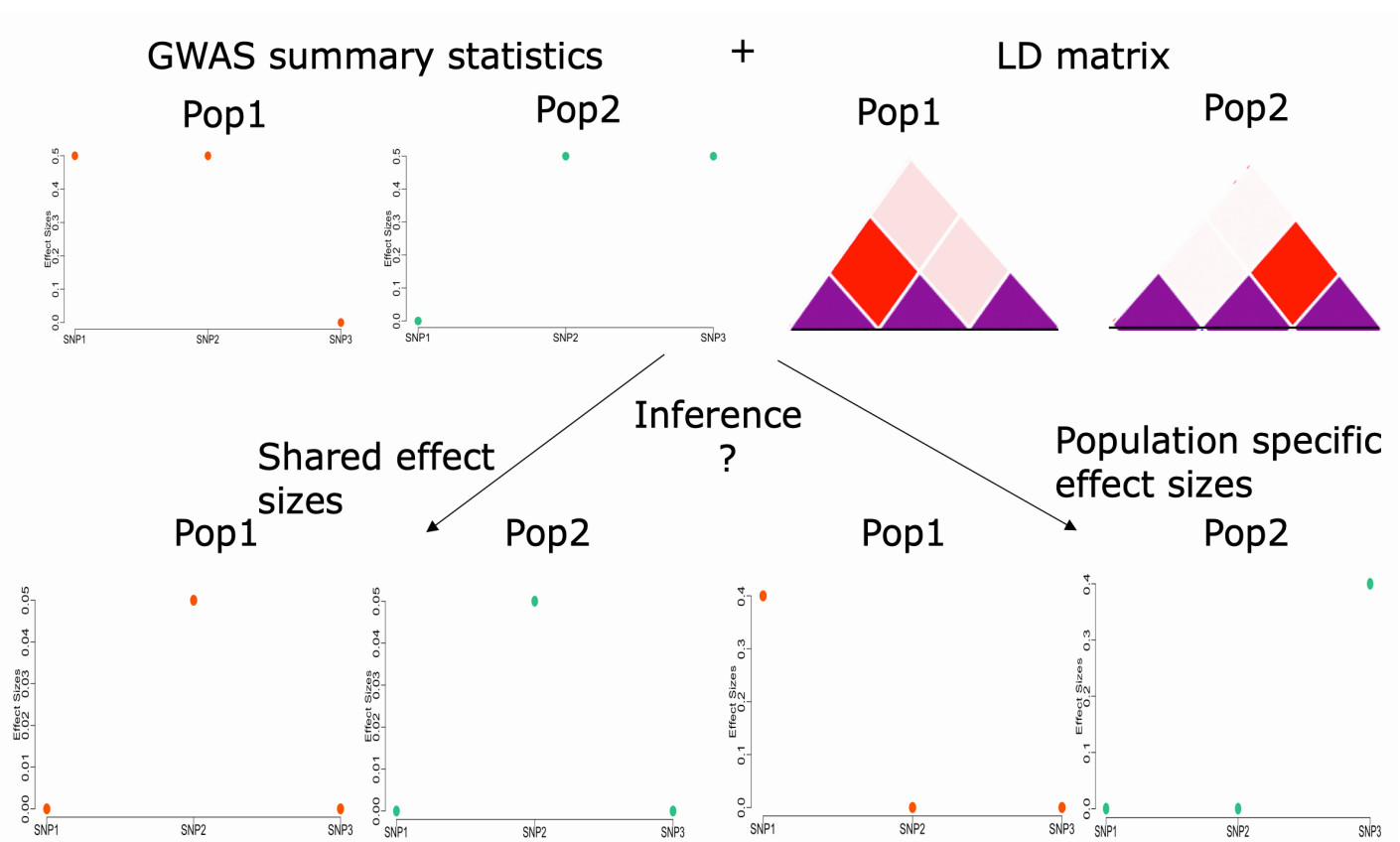
Figure S1. An example of identifiability issue caused by difference of local LD pattern of SNPs in two populations. SNP 1 and SNP 2 are in LD and have similar marginal effect sizes in population 1, while SNP2 and SNP3 are in LD and have similar marginal effect sizes in population 2. Two scenarios are likely to explain the observed GWAS summary statistics, which is not locally identifiable. In the first scenario, SNP 2 is causal and effect sizes are shared between populations. In the second scenario, SNP 1 is causal in population 1 and SNP 3 is causal in population 2. If genetic effects for most SNPs are shared between populations, then inference leading to population specific effect sizes would under-estimate the proportion of SNPs with shared effects and result in the loss of prediction accuracy.
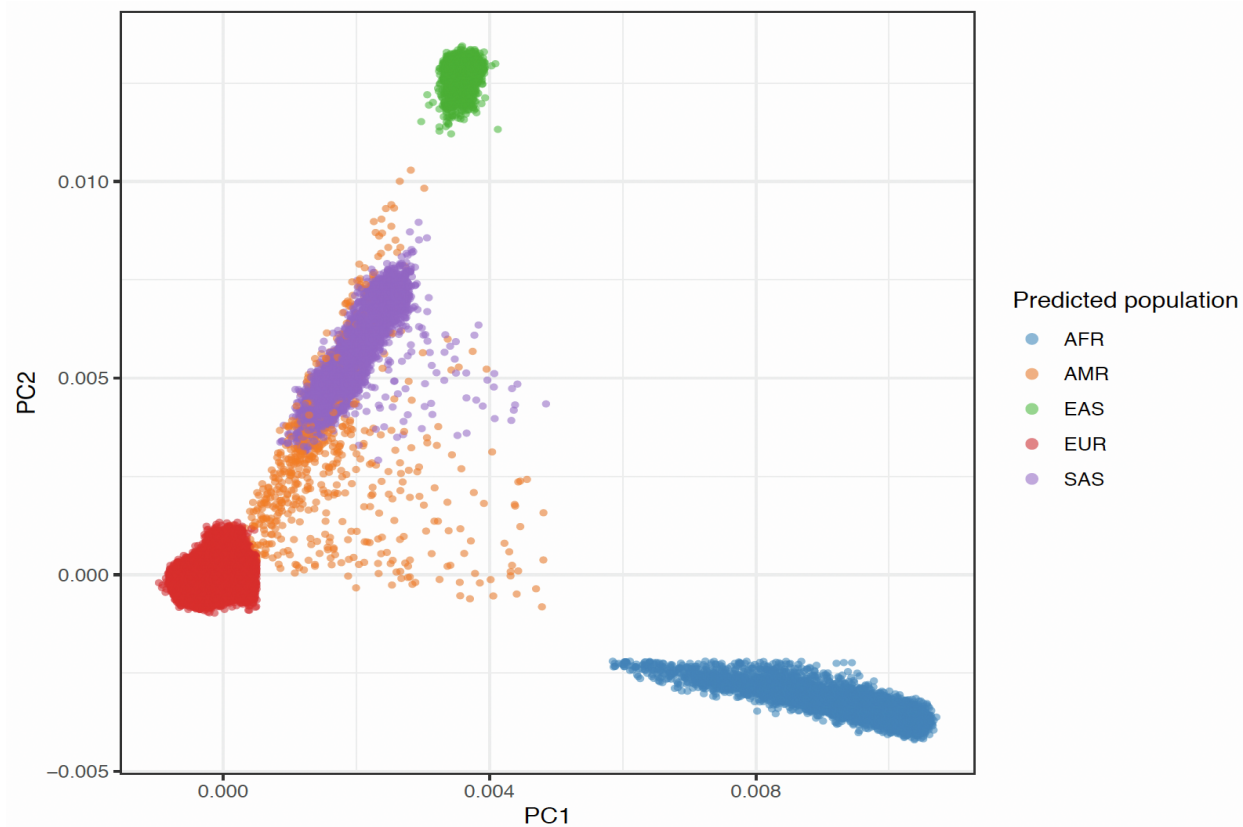
Figure S2. Principal component analysis of UK Biobank individuals after the assignment to one of five super populations (European, East Asian, African, Admixed American, South Asian) by a random forest classifier. We retained 2091 unrelated EAS and 6829 unrelated AFR samples with a predicted probability greater than 0.9 to form the validation and test datasets.
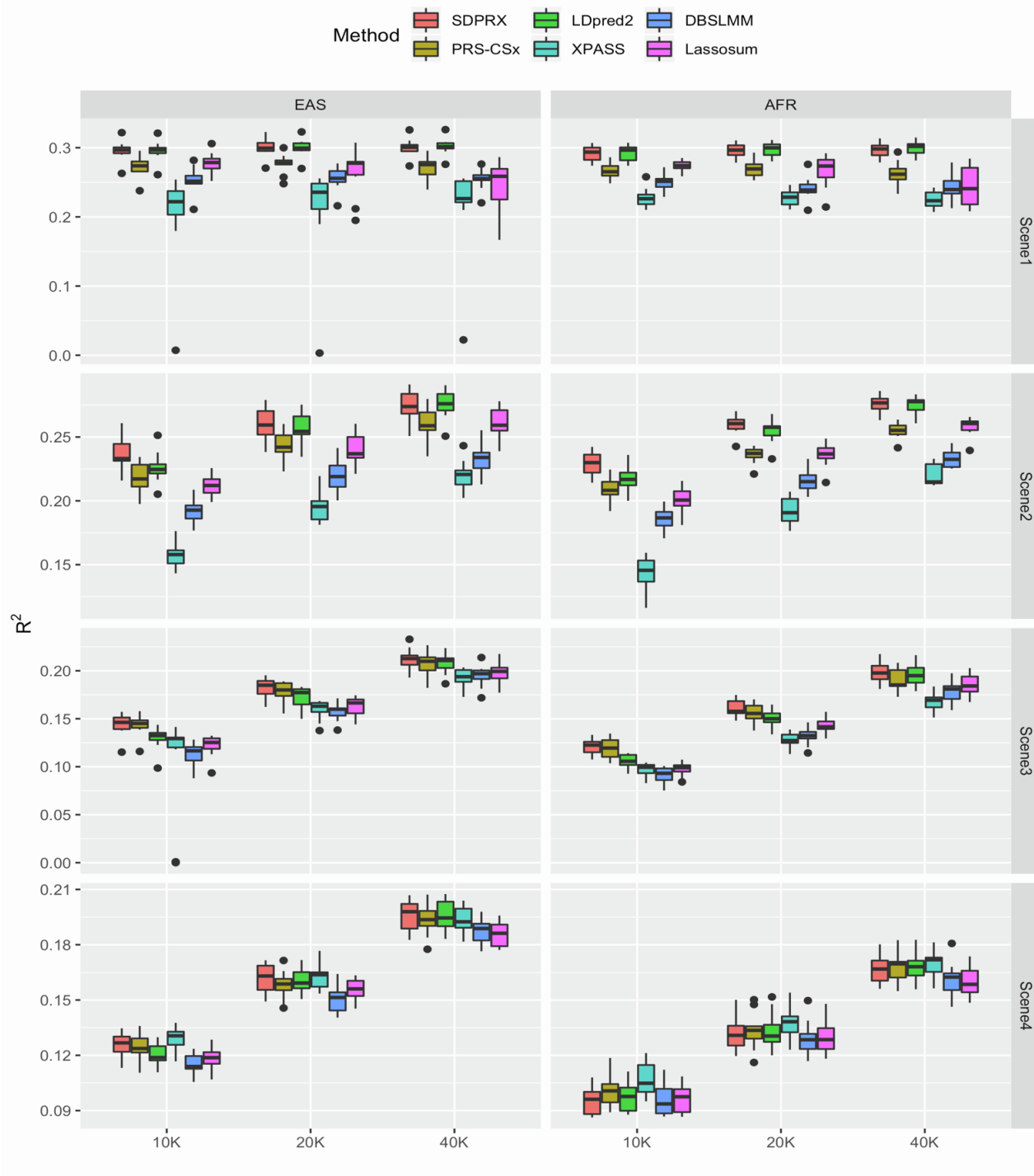
Figure S3. Prediction performance of different methods on simulated data. The proportion of

SNPs with population 1 specific, population 2 specific and correlated effect sizes was equally set

to be 0.05% (Scenario 1), 0.5% (Scenario 2) and 5% (Scenario 3). For Scenario 4, the proportion

of SNPs with population 1 specific, population 2 specific effect sizes were set to 5% and the proportion of SNPs with shared effect sizes was set to 90%. The cross-population genetic correlation was set to be 0.6 and the heritability was 0.3. Simulation in each scenario was repeated for 10 times. For each boxplot, the central mark is the median and the lower and upper edges represent the 25th and 75th percentiles.
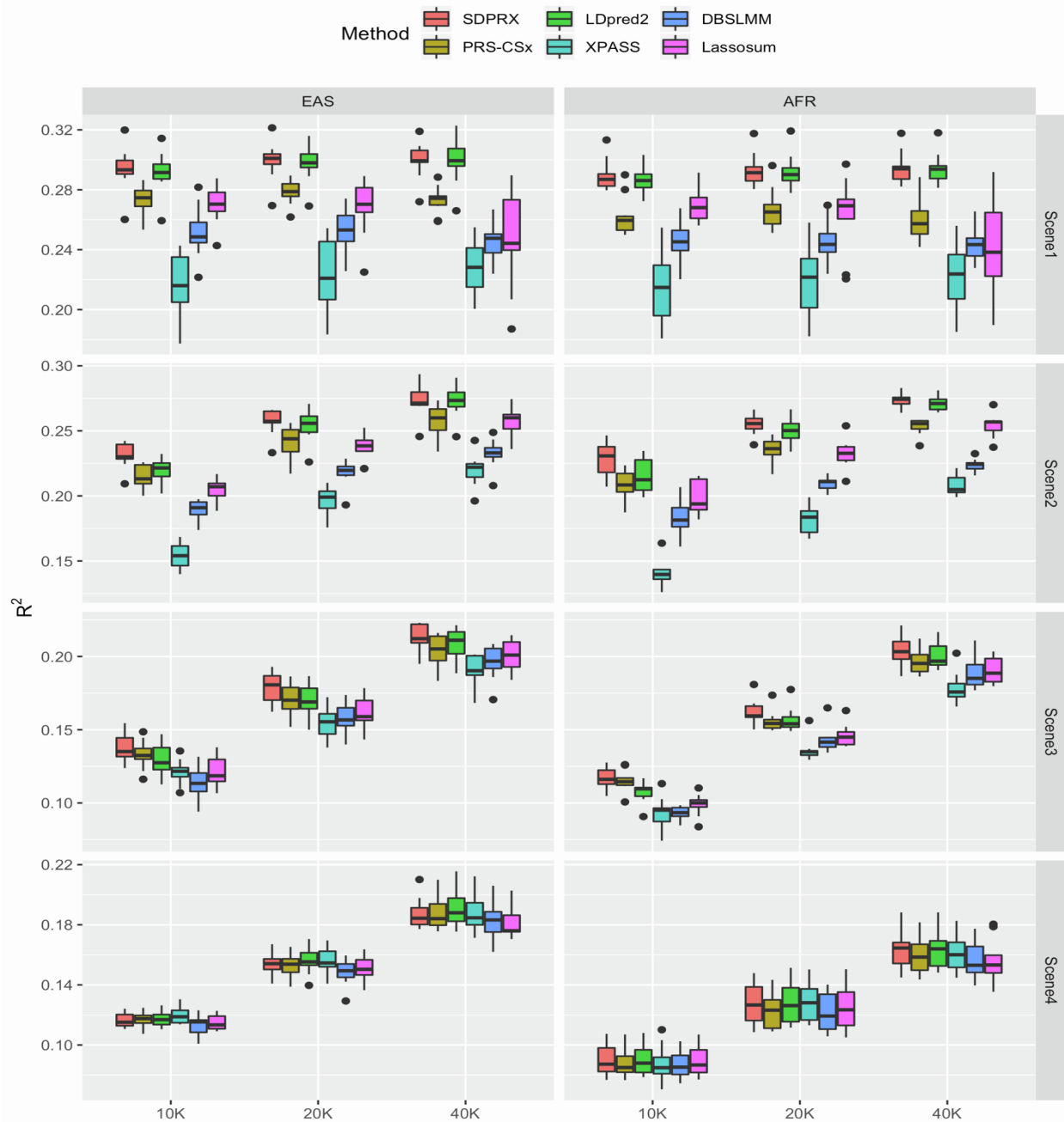
Figure S4. Prediction performance of different methods on simulated data. The proportion of

SNPs with population 1 specific, population 2 specific and correlated effect sizes was equally set

to be 0.05% (Scenario 1), 0.5% (Scenario 2) and 5% (Scenario 3). For Scenario 4, the proportion

of SNPs with population 1 specific, population 2 specific effect sizes were set to 5% and the

proportion of SNPs with shared effect sizes was set to 90%. The cross-population genetic

correlation was set to be 0.4 and the heritability was 0.3. Simulation in each scenario was

repeated for 10 times. For each boxplot, the central mark is the median and the lower and

upper edges represent the 25th and 75th percentiles.
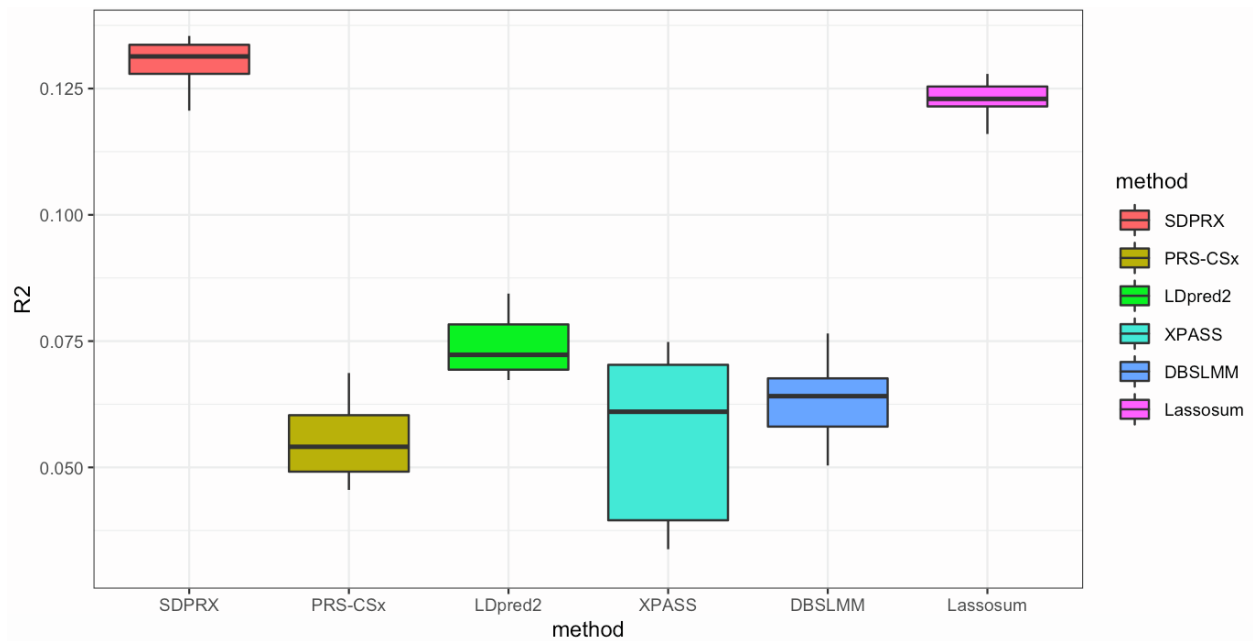
Figure S5. Prediction performance of different methods on simulated data for admixed individuals. The proportion of SNPs with population 1 specific, population 2 specific and correlated effect sizes was equally set to be 5% (Scenario 3). The cross-population genetic correlation was set to be 0.8 and the heritability was 0.4. The sample size was 40K for both EUR and AMR individuals. Simulation in each scenario was repeated for 10 times. For each boxplot, the central mark is the median and the lower and upper edges represent the 25th and 75th percentiles.
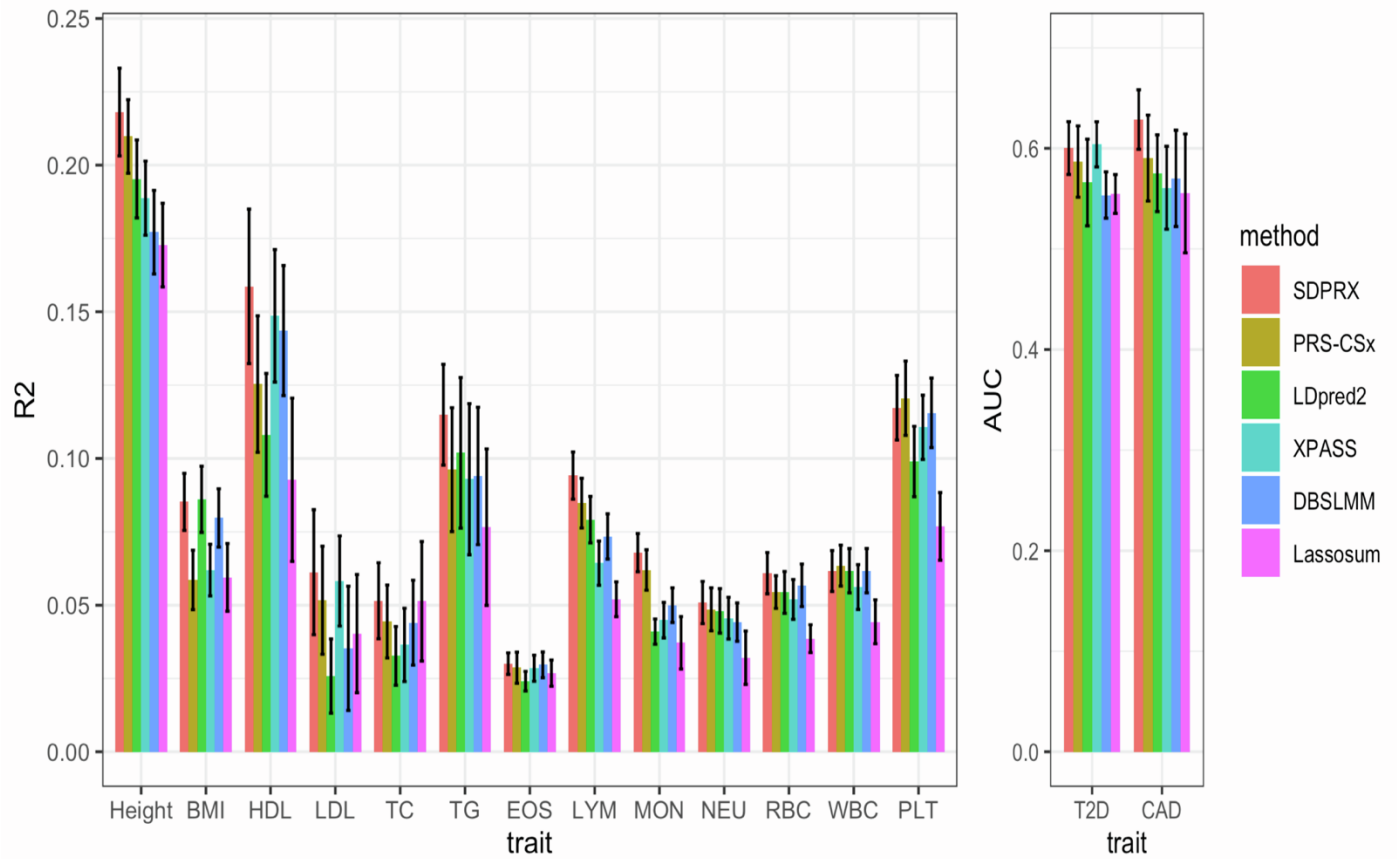
Figure S6. Prediction performance of different methods for 15 quantitative traits and 2 binary traits in EAS samples from UK Biobank with the linear combination of effect sizes. Selected participants with corresponding phenotypes were randomly split to form the validation (1/3) and test datasets (2/3). The mean and standard deviation of R^2 (quantitative trait) and AUC (binary trait) across 20 random splits are showed on the bar plots.
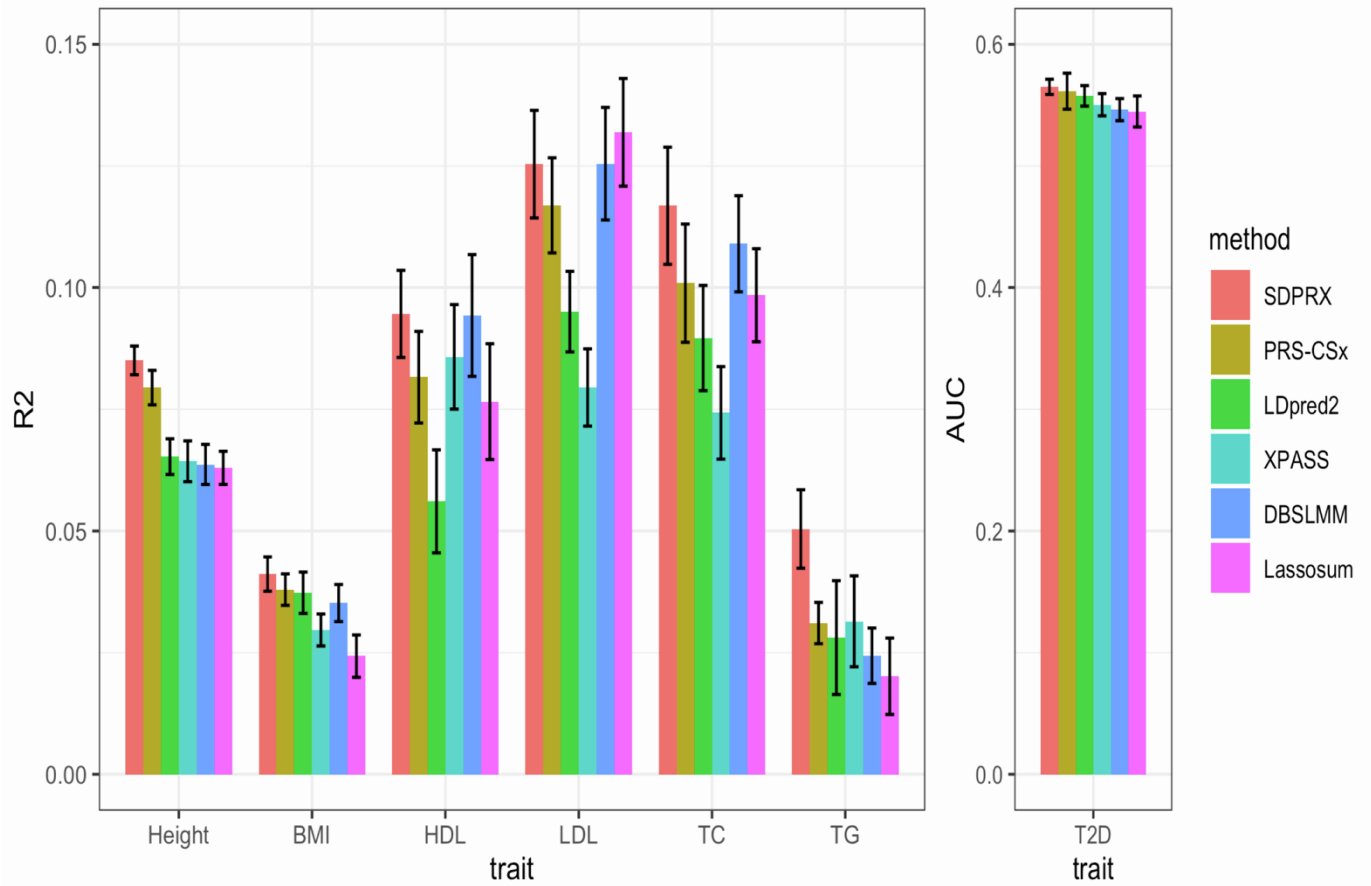
Figure S7. Prediction performance of different methods for 6 quantitative traits and 1 binary trait in AFR samples from UK Biobank with the linear combination of effect sizes. Selected participants with corresponding phenotypes were randomly split to form the validation (1/3) and test dataset (2/3). The mean and standard deviation of R^2 (quantitative trait) and AUC (binary trait) across 20 random splits are showed on the bar plots.
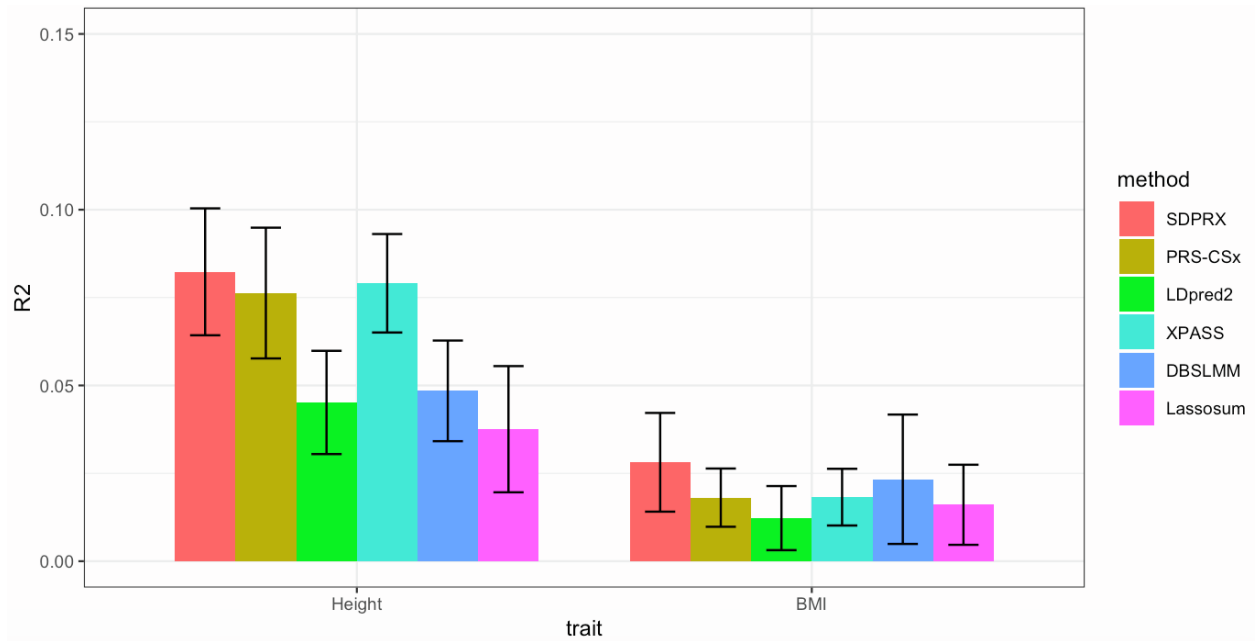
Figure S8. Prediction performance of different methods for 2 quantitative traits in AMR samples from UK Biobank. Selected participants with corresponding phenotypes were randomly split to form the validation (1/3) and test dataset (2/3). The mean and standard deviation of R^2 (quantitative trait) across 20 random splits are showed on the bar plots.

Supplementary Tables

|		EAS			AFR		
		10K	20K	40K	10K	20K	40K
Scene 1	SDPRX	0.290	0.292	0.294	0.292	0.294	0.294
	PRS-CSx	0.268	0.274	0.274	0.263	0.268	0.261
	LDpred2	0.290	0.293	0.296	0.292	0.292	0.294
	XPASS	0.224	0.231	0.233	0.225	0.231	0.231
	DBSLMM	0.250	0.256	0.250	0.246	0.244	0.240
	Lassosum	0.270	0.276	0.256	0.269	0.270	0.231
Scene 2	SDPRX	0.230	0.259	0.271	0.229	0.258	0.274
	PRS-CSx	0.219	0.240	0.255	0.210	0.236	0.253
	LDpred2	0.222	0.257	0.269	0.219	0.252	0.273
	XPASS	0.156	0.199	0.221	0.140	0.182	0.213
	DBSLMM	0.189	0.220	0.232	0.181	0.208	0.226
	Lassosum	0.204	0.238	0.253	0.201	0.239	0.262
Scene 3	SDPRX	0.145	0.184	0.214	0.131	0.169	0.208
	PRS-CSx	0.153	0.183	0.209	0.136	0.166	0.196
	LDpred2	0.127	0.171	0.207	0.108	0.154	0.200
	XPASS	0.135	0.164	0.193	0.111	0.140	0.173
	DBSLMM	0.111	0.164	0.199	0.090	0.137	0.183
	Lassosum	0.120	0.161	0.197	0.097	0.144	0.191
Scene 4	SDPRX	0.142	0.174	0.197	0.103	0.135	0.168
	PRS-CSx	0.134	0.167	0.200	0.103	0.135	0.169
	LDpred2	0.122	0.163	0.195	0.092	0.131	0.167
	XPASS	0.131	0.169	0.196	0.107	0.141	0.171
	DBSLMM	0.117	0.149	0.190	0.903	0.128	0.161
	Lassosum	0.122	0.159	0.187	0.089	0.126	0.159

Table S1. The median of square of Pearson correlation across 10 replications when the cross-population genetic correlation was 0.8.

		EAS			AFR		
		10K	20K	40K	10K	20K	40K
Scene 1	SDPRX	0.297	0.299	0.301	0.294	0.297	0.298
	PRS-CSx	0.274	0.278	0.276	0.265	0.269	0.262
	LDpred2	0.297	0.299	0.302	0.297	0.300	0.302
	XPASS	0.222	0.236	0.226	0.226	0.228	0.223
	DBSLMM	0.252	0.256	0.255	0.251	0.239	0.240
	Lassosum	0.279	0.278	0.259	0.274	0.274	0.241
Scene 2	SDPRX	0.233	0.259	0.274	0.230	0.260	0.277
	PRS-CSx	0.217	0.242	0.259	0.208	0.237	0.255
	LDpred2	0.225	0.254	0.276	0.217	0.258	0.278
	XPASS	0.158	0.196	0.221	0.146	0.191	0.215
	DBSLMM	0.193	0.219	0.234	0.187	0.215	0.232
	Lassosum	0.212	0.237	0.259	0.201	0.237	0.261
Scene 3	SDPRX	0.146	0.185	0.213	0.123	0.158	0.198
	PRS-CSx	0.145	0.180	0.210	0.119	0.156	0.185
	LDpred2	0.134	0.178	0.211	0.106	0.150	0.195
	XPASS	0.130	0.163	0.194	0.096	0.127	0.169
	DBSLMM	0.117	0.160	0.197	0.093	0.132	0.181
	Lassosum	0.125	0.167	0.199	0.099	0.142	0.184
Scene 4	SDPRX	0.127	0.163	0.198	0.096	0.131	0.167
	PRS-CSx	0.124	0.159	0.194	0.101	0.134	0.170
	LDpred2	0.119	0.159	0.195	0.098	0.130	0.168
	XPASS	0.131	0.164	0.192	0.105	0.138	0.172
	DBSLMM	0.114	0.151	0.189	0.094	0.128	0.162
	Lassosum	0.119	0.156	0.185	0.098	0.129	0.159

Table S2. The median of square of Pearson correlation across 10 replications when the cross-population genetic correlation was 0.6.

		EAS			AFR		
		10K	20K	40K	10K	20K	40K
Scene 1	SDPRX	0.294	0.301	0.299	0.287	0.291	0.294
	PRS-CSx	0.275	0.279	0.274	0.260	0.265	0.257
	LDpred2	0.292	0.298	0.300	0.286	0.290	0.294
	XPASS	0.216	0.221	0.228	0.215	0.222	0.224
	DBSLMM	0.245	0.254	0.248	0.245	0.244	0.243
	Lassosum	0.270	0.270	0.244	0.268	0.269	0.238
Scene 2	SDPRX	0.230	0.257	0.271	0.231	0.256	0.274
	PRS-CSx	0.213	0.244	0.260	0.208	0.236	0.256
	LDpred2	0.222	0.260	0.273	0.212	0.250	0.271
	XPASS	0.154	0.199	0.222	0.140	0.184	0.205
	DBSLMM	0.191	0.220	0.233	0.181	0.211	0.224
	Lassosum	0.207	0.238	0.260	0.194	0.233	0.257
Scene 3	SDPRX	0.135	0.181	0.212	0.116	0.159	0.203
	PRS-CSx	0.132	0.170	0.205	0.115	0.154	0.195
	LDpred2	0.123	0.169	0.211	0.109	0.154	0.197
	XPASS	0.122	0.155	0.190	0.095	0.135	0.176
	DBSLMM	0.113	0.157	0.197	0.093	0.142	0.185
	Lassosum	0.119	0.159	0.201	0.100	0.145	0.189
Scene 4	SDPRX	0.115	0.154	0.184	0.087	0.127	0.165
	PRS-CSx	0.118	0.154	0.184	0.085	0.123	0.158
	LDpred2	0.117	0.155	0.188	0.088	0.126	0.164
	XPASS	0.119	0.155	0.185	0.085	0.128	0.160
	DBSLMM	0.115	0.149	0.183	0.085	0.193	0.153
	Lassosum	0.113	0.150	0.176	0.087	0.123	0.153

Table S3. The median of square of Pearson correlation across 10 replications when the cross-population genetic correlation was 0.4.

Traits	SDPRX	PRS-CSx	LDpred2	XPASS	DBSLMM	Lassosum
Height	0.213	0.173	0.174	0.171	0.152	0.144
BMI	0.085	0.060	0.071	0.062	0.066	0.071
HDL	0.159	0.117	0.102	0.131	0.106	0.069
LDL	0.066	0.048	0.040	0.061	0.033	0.033
Total cholesterol	0.043	0.039	0.040	0.044	0.035	0.030
Log triglycerides	0.123	0.080	0.080	0.085	0.066	0.051
Eosinophils	0.031	0.027	0.013	0.014	0.028	0.014
Lymphocytes	0.096	0.063	0.039	0.037	0.053	0.025
Monocytes	0.057	0.056	0.039	0.025	0.032	0.035
Neutrophils	0.049	0.044	0.018	0.028	0.041	0.015
Red blood cell	0.061	0.050	0.031	0.036	0.051	0.033
White blood cell	0.062	0.052	0.029	0.035	0.050	0.025
Platelet	0.117	0.103	0.075	0.072	0.097	0.071
Coronary Artery disease	0.626	0.56	0.600	0.589	0.562	0.613
Type 2 diabetes	0.606	0.604	0.573	0.585	0.560	0.536

Table S4. The mean of variance of phenotypes explained by PRS for 13 quantitative traits and

AUC for 2 binary traits in EAS across 20 random splits without the linear combination of effect

sizes.

Traits	SDPRX	PRS-CSx	LDpred2	XPASS	DBSLMM	Lassosum
Height	0.218	0.210	0.195	0.189	0.177	0.173
BMI	0.085	0.059	0.086	0.062	0.080	0.059
HDL	0.159	0.126	0.108	0.149	0.144	0.093
LDL	0.061	0.052	0.026	0.058	0.035	0.041
Total cholesterol	0.051	0.044	0.033	0.036	0.044	0.051
Log triglycerides	0.115	0.096	0.102	0.093	0.094	0.077
Eosinophils	0.030	0.029	0.024	0.028	0.030	0.027
Lymphocytes	0.094	0.085	0.079	0.064	0.073	0.052
Monocytes	0.068	0.062	0.041	0.045	0.050	0.037
Neutrophils	0.051	0.049	0.048	0.046	0.044	0.032
Red blood cell	0.061	0.054	0.054	0.052	0.057	0.039
White blood cell	0.062	0.064	0.062	0.056	0.062	0.044
Platelet	0.117	0.121	0.099	0.110	0.116	0.077
Coronary Artery disease	0.629	0.590	0.575	0.561	0.570	0.555
Type 2 diabetes	0.600	0.587	0.566	0.604	0.554	0.555

Table S5. The mean of variance of phenotypes explained by PRS for 13 quantitative traits and

AUC for 2 binary traits in EAS across 20 random splits with the linear combination of effect

sizes.

Traits	SDPRX	PRS-CSx	LDpred2	XPASS	DBSLMM	Lassosum
Height	0.083	0.061	0.051	0.054	0.041	0.038
BMI	0.041	0.025	0.023	0.028	0.021	0.019
HDL	0.095	0.082	0.090	0.083	0.082	0.088
LDL	0.128	0.120	0122	0.079	0.125	0.128
Total cholesterol	0.124	0.102	0.123	0.074	0.108	0.119
Log triglycerides	0.051	0.036	0.038	0.032	0.038	0.025
Type 2 diabetes	0.560	0.551	0.544	0.548	0.539	0.536

Table S6. The mean of variance of phenotypes explained by PRS for six quantitative traits and

AUC for one binary trait in AFR across 20 random splits without the linear combination of effect

sizes.

Traits	SDPRX	PRS-CSx	LDpred2	XPASS	DBSLMM	Lassosum
Height	0.085	0.079	0.065	0.064	0.064	0.063
BMI	0.041	0.038	0.037	0.030	0.035	0.024
HDL	0.095	0.082	0.056	0.086	0.094	0.077
LDL	0.125	0.117	0.095	0.079	0.125	0.132
Total cholesterol	0.117	0.101	0.090	0.074	0.109	0.098
Log triglycerides	0.050	0.031	0.028	0.031	0.024	0.020
Type 2 diabetes	0.565	0.561	0.558	0.550	0.546	0.545

Table S7. The mean of variance of phenotypes explained by PRS for six quantitative traits and

AUC for one binary trait in AFR across 20 random splits with the linear combination of effect

sizes.

Traits	SDPRX	PRS-CSx	LDpred2	XPASS	DBSLMM	Lassosum
Height	9.8 (4.4)	6.2 (1.0)	1.1 (26.1)	0.3 (18.0)	0.8 (1.0)	0.1 (2.4)
BMI	8 (4.7)	5.5 (1.0)	1.1 (25.8)	0.3 (22.0)	1.0 (1.0)	0.1 (2.4)
HDL	8.5 (4.7)	5.2 (1.0)	0.9 (23.6)	0.3 (18.3)	0.9 (1.0)	0.1 (2.0)
LDL	8.5 (4.7)	5.3 (1.0)	1.1 (23.5)	0.2 (19.3)	0.9 (1.0)	0.1 (2.3)
TC	5.1 (4.0)	4.3 (1.0)	1.1 (23.6)	0.3 (14.8)	0.9 (1.0)	0.09 (1.6)
TG	8.5 (4.7)	4.3 (1.0)	1.2 (23.6)	0.3 (19.3)	0.6 (0.8)	0.1 (2.3)
EOS	8.4 (4.9)	5.4 (1.0)	1.0 (23.3)	0.3 (19.2)	0.9 (1.0)	0.1 (2.3)
LYM	8.5 (4.9)	5.5 (1.0)	1.3 (23.3)	0.3 (19.2)	0.9 (1.0)	0.1 (2.0)
MON	8.5 (4.9)	4.7 (1.0)	1.3 (23.3)	0.3 (19.2)	1.5 (1.0)	0.1 (2.0)
NEU	8.5 (4.9)	4.3 (1.0)	1.3 (23.3)	0.3 (19.2)	0.9 (1.0)	0.1 (2.0)
RBC	8.6 (4.9)	4.7 (1.0)	1.1 (23.3)	0.3 (19.2)	0.9 (1.0)	0.1 (2.3)
WBC	8.7 (4.8)	5.2 (1.0)	1.1 (23.3)	0.3 (19.2)	0.8 (1.0)	0.1 (2.3)
PLT	8.5 (4.9)	4.3 (1.0)	1.0 (23.3)	0.3 (19.2)	0.8 (1.0)	0.1 (2.0)
T2D	4.5 (4.2)	5.5 (1.0)	1.0 (14.9)	0.3 (15.9)	0.8 (0.9)	0.1 (1.7)
CAD	6.9 (4.5)	4.7 (0.9)	1.1 (22.3)	0.3 (17.4)	0.9 (0.9)	0.1 (2.5)

Table S8. Computational time and memory usage of different methods for 15 traits. The computational time is in hours. Memory usage of each method, as listed in the parenthesis, is measured in the unit of Gigabytes (Gb).

Supplemental Methods

MCMC Algorithm

Here we describe our MCMC algorithm based on Gibbs sampling to obtain the posterior samples. For each SNP j, we introduce a vector $z_j = (m, k), m \in \{0,1,2,3\}, k \in \{1,2,\ldots,1000\}$ indicating whether effect sizes are population specific and which variance component it is assigned to. For example, z_j equals (1,4) if the effect sizes of SNP j are population 1 specific and it is assigned to the fourth variance component.

Compute A_1, B_1, A_2, B_2: $A_1 = (R_1 + N_1 aI)^{-1} R_1$, $B_1 = R_1 A_1$. $A_2 = (R_2 + N_2 aI)^{-1} R_2$, $B_2 = R_2 A_2$.

Sampling z_j: For each LD block, we first integrate out $\boldsymbol{\beta_1}$ and $\boldsymbol{\beta_2}$ to derive the conditional probability of SNP j whose effect sizes are correlated in two populations and assigned to the kth variance component:

$$P\big(z_j = (3, k)\big|.\big)$$

$$\propto \int \int p(\widehat{\boldsymbol{\beta}}_1 | \boldsymbol{\beta}_{1j}, \eta) \, p(\widehat{\boldsymbol{\beta}}_2 | \boldsymbol{\beta}_{2j}, \eta) \, p(\boldsymbol{\beta}_{1j}, \boldsymbol{\beta}_{2j} | z_j = (3, k), \sigma_{3k}^2) \, d\beta_{1j} d\beta_{2j}$$

$$\times \; P\big(z_j = (3, k)\big)$$

$$\propto \int \int \exp\left\{-\frac{1}{2}\left(\widehat{\boldsymbol{\beta}}_1 - \eta \boldsymbol{R_1}\boldsymbol{\beta_1}\right)^T (\boldsymbol{R_1}/N_1 + a\boldsymbol{I})^{-1}\left(\widehat{\boldsymbol{\beta}}_1 - \eta \boldsymbol{R_1}\boldsymbol{\beta_1}\right)\right\}\exp\left\{-\frac{1}{2}\left(\widehat{\boldsymbol{\beta}}_2\right.\right.$$

$$\left. - \eta \boldsymbol{R_2}\boldsymbol{\beta_2}\right)^T (\boldsymbol{R_2}/N_2 + a\boldsymbol{I})^{-1}\left(\widehat{\boldsymbol{\beta}}_2\right.$$

$$\left.\left. - \eta \boldsymbol{R_2}\boldsymbol{\beta_2}\right)\right\}\frac{1}{2\pi\sigma_{3k}^2\sqrt{1-\rho^2}}\exp\left\{-\frac{1}{2(1-\rho^2)}\left[\frac{\beta_{1j}^2 + \beta_{2j}^2 - 2\rho\beta_{1j}\beta_{2j}}{\sigma_{3k}^2}\right]\right\}d\beta_{1j}d\beta_{2j}$$

$$\times \pi_{3k}p_3$$

$$\propto \int \int \exp\left\{-\frac{N_1}{2}\eta^2\boldsymbol{\beta_1^T}\boldsymbol{B_1}\boldsymbol{\beta_1} + N_1\eta\widehat{\boldsymbol{\beta}}_1^{\ T}\boldsymbol{A_1}\boldsymbol{\beta_1}\right\}\exp\left\{-\frac{N_2}{2}\eta^2\boldsymbol{\beta_2^T}\boldsymbol{B_2}\boldsymbol{\beta_2}\right.$$

$$\left. + N_2\eta\widehat{\boldsymbol{\beta}}_2^{\ T}\boldsymbol{A_2}\beta_{12}\right\}\frac{1}{2\pi\sigma_{3k}^2\sqrt{1-\rho^2}}\exp\left\{-\frac{1}{2(1-\rho^2)}\left[\frac{\beta_{1j}^2 + \beta_{2j}^2 - 2\rho\beta_{1j}\beta_{2j}}{\sigma_{3k}^2}\right]\right\}d\beta_{1j}d\beta_{2j}$$

$$\times \pi_{3k}p_3$$

$$\propto \int \int \exp\left\{-\frac{N_1}{2}\eta^2 B_{1,jj}\beta_{1j}^2 - N_1\eta^2 \sum_{i\neq j} B_{1,ij}\beta_{1i}\beta_{1j}\right.$$

$$\left. + N_1\eta \sum_i A_{1,ij}\hat{\beta}_{1i}\beta_{1j}\right\} \exp\left\{-\frac{N_2}{2}\eta^2 B_{2,jj}\beta_{2j}^2 - N_2\eta^2 \sum_{i\neq j} B_{2,ij}\beta_{2i}\beta_{2j}\right.$$

$$\left. + N_2\eta \sum_i A_{2,ij}\hat{\beta}_{2i}\beta_{2j}\right\}\frac{1}{2\pi\sigma_{3k}^2\sqrt{1-\rho^2}}\exp\left\{-\frac{1}{2(1-\rho^2)}\left[\frac{\beta_{1j}^2 + \beta_{2j}^2 - 2\rho\beta_{1j}\beta_{2j}}{\sigma_{3k}^2}\right]\right\}d\beta_{1j}d\beta_{2j}$$

$$\times \pi_{3k}p_3$$

$$\propto \int \int \exp\left\{-a_{jk1}\beta_{1j}^2 - a_{jk2}\beta_{2j}^2 + N_1 b_{1j} + N_2 b_{2j} + c_k\beta_{1j}\beta_{2j}\right\}\frac{1}{2\pi\sigma_{3k}^2\sqrt{1-\rho^2}}d\beta_{1j}d\beta_{2j}$$

$$\times \pi_{3k}p_3$$

$$\propto \frac{1}{\left(4a_{jk1}a_{jk2} - c_k^2\right)^{\frac{1}{2}}\sigma_{3k}^2}\exp\left\{a_{jk1}\mu_{jk1}^2 + a_{jk2}\mu_{jk2}^2 - c_k\mu_{jk1}\mu_{jk2}\right\}\times \frac{\pi_{3k}p_3}{\sqrt{1-\rho^2}}$$

$$(1)$$

where

$$b_{1j} = \eta \sum_i A_{1,ij} \hat{\beta}_{1i} - \eta^2 \sum_{i \neq j} B_{1,ij} \beta_{1i}$$

$$b_{2j} = \eta \sum_i A_{2,ij} \hat{\beta}_{2i} - \eta^2 \sum_{i \neq j} B_{2,ij} \beta_{2i}$$

$$a_{jk1} = \frac{N_1}{2} \eta^2 B_{1,jj} + \frac{1}{2\sigma_{3k}^2 (1 - \rho^2)}$$

$$a_{jk2} = \frac{N_2}{2} \eta^2 B_{2,jj} + \frac{1}{2\sigma_{3k}^2 (1 - \rho^2)}$$

$$\mu_{jk1} = \frac{2 a_{jk2} N_1 b_{1j} + c_k N_2 b_{2j}}{4 a_{jk1} a_{jk2} - c_k^2}$$

$$\mu_{jk2} = \frac{2 a_{jk1} N_2 b_{2j} + c_k N_1 b_{1j}}{4 a_{jk1} a_{jk2} - c_k^2}$$

$$c_k = \frac{\rho}{(1 - \rho^2)\sigma_{3k}^2}$$

We next derive the conditional probability of SNP j whose effect sizes are population specific or null. It can be viewed as the special case to evaluate the last integrand by setting $\rho = 0, \beta_{2j} = 0$ (population 1 specific), $\rho = 0, \beta_{1j} = 0$ (population 2 specific), and $\beta_{1j} = \beta_{2j} = 0$ (both null).

$$P(z_j = (1,k)|.) \propto \frac{1}{\sqrt{N_1 \eta^2 B_{1,jj} \sigma_{1k}^2 + 1}} \exp\left\{\frac{N_1^2 b_{1j}^2}{2(N_1 \eta^2 B_{1,jj} + \sigma_{1k}^{-2})}\right\} \times \pi_{1k} p_1$$

$$P(z_j = (2,k)|.) \propto \frac{1}{\sqrt{N_2 \eta^2 B_{2,jj} \sigma_{2k}^2 + 1}} \exp\left\{\frac{N_2^2 b_{2j}^2}{2(N_2 \eta^2 B_{2,jj} + \sigma_{2k}^{-2})}\right\} \times \pi_{2k} p_2$$

$$P(z_j = (0,0)|.) \propto p_0$$

We use log-exp-sum trick to avoid numerical overflow. Note that because SNPs in different LD blocks are approximately independent, we can sample their assignments in parallel. For population 1 specific SNPs, we only need to evaluate $P\left(z_j = (1,k)|.\right)$ and $P\left(z_j = (0,0)|.\right)$.

Sampling $\boldsymbol{\beta_1}, \boldsymbol{\beta_2}$: For SNPs that are non-causal in any populations, we simply set the corresponding entries of $\boldsymbol{\widehat{\beta}_1}$ and $\boldsymbol{\widehat{\beta}_2}$ as zero. We then jointly sample the effect sizes of causal SNPs in one independent LD block. We introduce two indexes γ_1 and γ_2 such that $\boldsymbol{\beta_{1,\gamma_1}}$ and $\boldsymbol{\beta_{2,\gamma_2}}$ are non-zero. We combine $\boldsymbol{\beta_{1,\gamma_1}}$ and $\boldsymbol{\beta_{2,\gamma_2}}$ into one vector $\boldsymbol{\beta_\gamma}$, which follows a bivariate normal distribution with mean 0 and variance-covariance matrix $\boldsymbol{\Sigma_0}$. The jth diagonal entry of $\boldsymbol{\Sigma_0}$ is $\sigma_{z_j}^2$. If effect sizes of one SNP are non-zero with correlation in two populations, then $\Sigma_{0,ij} = \Sigma_{0,ji} = \rho\sigma_{z_j}^2$. Other entries of Σ_0 are zero. Note that the special structure of $\boldsymbol{\Sigma_0}$ allows an analytical solution of $\boldsymbol{\Sigma_0^{-1}}$. We next derive the conditional likelihood as:

$$p\left(\boldsymbol{\beta_{1,\gamma_1}}, \boldsymbol{\beta_{2,\gamma_2}}|.\right)$$

$$\propto \exp\left\{-\frac{N_1}{2}\eta^2\boldsymbol{\beta_1^T}B_1\boldsymbol{\beta_1}\right.$$

$$\left.+ \eta\boldsymbol{\widehat{\beta}_1}^T A_1\boldsymbol{\beta_1}\right\}\exp\left\{-\frac{N_2}{2}\eta^2\boldsymbol{\beta_2^T}B_2\boldsymbol{\beta_2} + \eta\boldsymbol{\widehat{\beta}_2}^T A_2\boldsymbol{\beta_2}\right\}\exp\left\{-\frac{1}{2}\left(\boldsymbol{\beta_{1,\gamma_1}}\ \boldsymbol{\beta_{2,\gamma_2}}\right)^T\Sigma_0^{-1}\left(\boldsymbol{\beta_{1,\gamma_1}}\ \boldsymbol{\beta_{2,\gamma_2}}\right)\right\}$$

$$\propto \exp\left\{-\frac{1}{2}\eta^2\left(\boldsymbol{\beta_{1,\gamma_1}}\ \boldsymbol{\beta_{2,\gamma_2}}\right)^T\begin{pmatrix}N_1B_{1,\gamma_1} & 0\\ 0 & N_2B_{2,\gamma_2}\end{pmatrix}\left(\boldsymbol{\beta_{1,\gamma_1}}\ \boldsymbol{\beta_{2,\gamma_2}}\right)\right.$$

$$\left.+ \eta\left(N_1\boldsymbol{\widehat{\beta}_1^T}A_{1,\gamma_1}\quad N_2\boldsymbol{\widehat{\beta}_2^T}A_{2,\gamma_2}\right)\right\}\exp\left\{-\frac{1}{2}\left(\boldsymbol{\beta_{1,\gamma_1}}\ \boldsymbol{\beta_{2,\gamma_2}}\right)^T\Sigma_0^{-1}\left(\boldsymbol{\beta_{1,\gamma_1}}\ \boldsymbol{\beta_{2,\gamma_2}}\right)\right\}$$

$$\propto \exp\left\{-\frac{1}{2}\eta^2\boldsymbol{\beta_\gamma^T}B_\gamma\boldsymbol{\beta_\gamma} + \eta\boldsymbol{\widehat{\beta}^T}A_\gamma\boldsymbol{\beta_\gamma}\right\}\exp\left\{-\frac{1}{2}\boldsymbol{\beta_\gamma^T}\Sigma_0^{-1}\boldsymbol{\beta_\gamma}\right\}$$

$$= MVN(\eta \Sigma A_\gamma^T \widehat{\boldsymbol{\beta}}_\gamma, \Sigma)$$

$$(2)$$

where $\Sigma = \left(\eta^2 B_\gamma + \Sigma_0^{-1} \right)^{-1}$, $A_\gamma = \left(N_1 \widehat{\boldsymbol{\beta}}_1^T A_{1,\gamma_1} \quad N_2 \widehat{\boldsymbol{\beta}}_2^T A_{2,\gamma_2} \right)$, $B_\gamma = \begin{pmatrix} N_1 B_{1,\gamma_1} & 0 \\ 0 & N_2 B_{2,\gamma_2} \end{pmatrix}$. A_{1,γ_1}

is the submatrix by selecting columns from matrices A_1 based on the index γ_1. B_{1,γ_1} is the

submatrix by selecting rows and columns from matrices B_1 based on the index γ_1.

Sampling η: The full conditional likelihood is

$$p(\eta|.)$$

$$\propto \exp\left\{ -\frac{1}{2} N_1 \eta^2 \sum \boldsymbol{\beta}_1^T B_1 \boldsymbol{\beta}_1 \right.$$

$$\left. + N_1 \eta \sum \widehat{\boldsymbol{\beta}}_1^T A_1 \boldsymbol{\beta}_1 \right\} \exp\left\{ -\frac{1}{2} N_2 \eta^2 \sum \boldsymbol{\beta}_2^T B_2 \boldsymbol{\beta}_2 + N_2 \eta \sum \widehat{\boldsymbol{\beta}}_2^T A_2 \boldsymbol{\beta}_2 \right\} \exp\left\{ -\frac{\eta^2}{2 \times 10^{-6}} \right\}$$

$$= N\left(\frac{N_1(\sum \widehat{\boldsymbol{\beta}}_1^T A_1 \boldsymbol{\beta}_1) + N_2(\sum \widehat{\boldsymbol{\beta}}_2^T A_2 \boldsymbol{\beta}_2)}{N_1(\sum \boldsymbol{\beta}_1^T B_1 \boldsymbol{\beta}_1) + N_2(\sum \boldsymbol{\beta}_2^T B_2 \boldsymbol{\beta}_2) + 10^{-6}}, \frac{1}{N_1(\sum \boldsymbol{\beta}_1^T B_1 \boldsymbol{\beta}_1) + N_2(\sum \boldsymbol{\beta}_2^T B_2 \boldsymbol{\beta}_2) + 10^{-6}} \right)$$

Sampling $\sigma_{1k}^2, \sigma_{2k}^2, \sigma_{3k}^2$: The full conditional likelihood is

$$p(\sigma_{1k}^2|.) \propto \prod_{j:z_j=(1,k)} \frac{1}{\sigma_{1k}} \exp\left\{ -\frac{\beta_{1j}^2}{2\sigma_{1k}^2} \right\} \sigma_{1k}^{-2(.5-1)} \exp\left\{ -\frac{.5}{\sigma_{1k}^2} \right\}$$

$$= IG\left(\frac{M_{1k}}{2} + .5, \frac{\sum_{j:z_j=(1,k)} \beta_{1j}^2}{2} + .5 \right)$$

$$p(\sigma_{2k}^2|.) \propto \prod_{j:z_j=(2,k)} \frac{1}{\sigma_{2k}} \exp\left\{-\frac{\beta_{2j}^2}{2\sigma_{2k}^2}\right\} \sigma_{2k}^{-2(.5-1)} \exp\left\{-\frac{.5}{\sigma_{2k}^2}\right\}$$

$$= IG\left(\frac{M_{2k}}{2} + .5, \frac{\sum_{j:z_j=(2,k)} \beta_{2j}^2}{2} + .5\right)$$

$$p(\sigma_{3k}^2|.) \propto \prod_{j:z_j=(3,k)} \frac{1}{\sigma_{3k}} \exp\left\{-\frac{\beta_{1j}^2 + \beta_{2j}^2 - 2\rho\beta_{1j}\beta_{2j}}{2(1-\rho^2)\sigma_{3k}^2}\right\} \sigma_{3k}^{-2(.5-1)} \exp\left\{-\frac{.5}{\sigma_{3k}^2}\right\}$$

$$= IG\left(\frac{M_{3k}}{2} + .5, \frac{\sum_{j:z_j=(3,k)} \beta_{1j}^2 + \beta_{2j}^2 - 2\rho\beta_{1j}\beta_{2j}}{2(1-\rho^2)} + .5\right)$$

where $M_{1k} = \sum_j I\left(z_j = (1,k)\right)$, $M_{2k} = \sum_j I\left(z_j = (2,k)\right)$, $M_{3k} = \sum_j I\left(z_j = (3,k)\right)$ and I is the indicator function.

Sampling V_{mk}, $m \in \{1,2,3\}$, $k \in \{1,2,\dots,1000\}$: The full conditional likelihood is

$$p(V_{mk}|.) \propto V_k^{M_{mk}} (1-V_k)^{M_{m(k+1)} + \cdots + M_{1000} + \alpha_M - 1}$$

$$= Beta\left(1 + M_{mk}, \alpha + \sum_{l=k+1}^{1000} M_{ml}\right)$$

for j=1,2,3 and k = 1, …, 999. V_{m1000} equals 1 according to the definition of the truncated stick-breaking process.

Computing π_{mk}, $m \in \{1,2,3\}$: The prior probability can be computed as

$$\pi_{m1} = V_{m1}$$

$$\pi_{mk} = \prod_{l=1}^{k-1} (1 - V_{ml}) V_{mk} \quad (k \geq 2)$$

Sampling p_0, p_1, p_2, p_3: The conditional distribution is:

$$p_0, p_1, p_2, p_3 | . \sim Dir(M_0 + 1, M_1 + 1, M_2 + 1, M_3 + 1)$$

where $M_0 = \sum_j I\left(z_j = (0,0)\right), M_1 = \sum_j I\left(z_j = (1,.)\right), M_2 = \sum_j I\left(z_j = (2,.)\right), M_{3k} = \sum_j I\left(z_j = (3,.)\right)$. Note that we exclude population specific variants when computing M_0, M_1, M_2, M_3.

Sampling $\alpha_m, m \in \{1,2,3\}$: The full conditional likelihood is

$$p(\alpha_m | .) \propto \prod_{l=1}^{1000-1} \alpha_m (1 - V_{ml})^{\alpha_m - 1} \alpha_m^{.1-1} \exp\{-.1 \times \alpha_m\}$$

$$= Gamma(0.1 + 1000 - 1, 0.1 - \sum_{k=1}^{1000-1} \log(1 - V_{mk}))$$

We record the effect sizes $\eta\boldsymbol{\beta_1}$ and $\eta\boldsymbol{\beta_2}$ together with the heritability $h_1^2 = \boldsymbol{\beta_1^T R_1 \beta_1}$ and $h_2^2 = \boldsymbol{\beta_2^T R_2 \beta_2}$ for each iteration and compute the average of all posterior samples as the final estimator. We note that h_1^2 and h_2^2 together with the maximum of effect sizes can be used to assess whether the algorithm converges.